Reconstructing the *Tetrastichia bupatides* Gordon plant; a Devonian - Mississippian hydrasperman gymnosperm from Oxroad Bay, Scotland and Ballyheigue, Ireland

Gar W. Rothwell[1,*] Michael T. Dunn[2], and Andrew C. Scott[3]

[1]Department of Environmental and Plant Biology, Ohio University, Athens, Ohio 45701, U.S.A. E-mail: rothwell@ohio.edu; and Department of Botany and Plant Pathology, Oregon State University, Corvallis, Oregon 97331, U.S.A. E-mail: rothwell@ohio.edu; rothwelg@oregonstate.edu

[2]Department of Agriculture, Biology and Health Sciences, Cameron University, Lawton, Oklahoma 73505, U.S.A. E-mail: michaeld@cameron.edu

[3]Department of Earth Sciences, Royal Holloway University of London, Egham, Surrey, TW20 0EX, UK. E-mail: a.scott@rhul.ac.uk

Running head: Reconstruction of *Tetrastichia bupatides*

Key Words: frond structure, organismal concept, ovulate cupule, pollen organ, seed fern

* Corresponding author.

E-mail addresses: rothwell@ohio.edu, gar.rothwell@oregonstate.edu (Gar Rothwell)

ABSTRACT

An organismal concept for the Late Devonian/Mississippian hydrasperman seed fern *Tetrastichia bupatides* is developed from specimens collected at Oxroad Bay, East Lothian Scotland and Ballyheigue, County Kerry, Ireland. Specimens include interconnected fragments of stems, frond rachides, pinnae, pinnules, roots, pollen organs with enclosed pre-pollen, and cupules, as well as dispersed ovules. Both morphological and anatomical features are documented. The plant produces an unbranched, upright stem with a branched taproot, and small adventitious roots at the base of the stem. Stems have a mesarch actinostele with sympodial protoxylem architecture. Phyllotaxis ranges from helical to opposite/decussate, with planar fronds that typically fork twice at the base, and then produce pinnules of the *Rhodea*-type. Compact aggregate pollen organs are attached distally on secondary rachides and are constructed of cruciately forking axes that terminate in inverted, round, simple synangia of six elongated microsporangia attached to a basal pad of tissue. Ovulate cupules of the *Calathospermum fimbriatum* type are attached at the base of the frond. Ovules possibly could be *Salpingostoma dasu* or *Eospermum oxroadense*. *Tetrastichia bupatides* is now one of the most completely reconstructed of all Devonian-Mississippian hydrasperman seed ferns, and the most ancient gymnosperm for which the pattern of rooting has been established. The occurrence of a taproot at the base of the stem suggests that the plant may exhibit bipolar growth derived from a cotyledonary embryo.

1. Introduction

The origin of gymnospermous biology is among the seminal innovations in the evolution of modern land plants, and is characterized by the indehiscent, integumented megasporangium (i.e., the ovule or seed; Stewart and Rothwell, 1993), coupled with pollination to facilitate gametophyte development and fertilization, and with abscission to facilitate dispersal of the propagule (Rothwell and Scheckler, 1988). Additional features that characterize modern gymnosperms include post-zygotic quiescence (seed dormancy; Mapes, et al., 1989), bipolar growth from a cotyledonary embryo (Rothwell and Serbet, 1994), open repetitive growth architecture (Hallé et al., 1978), shoots with fully evolved stem, leaf, root organography (Sanders et al., 2009), sympodial protoxylem architecture of the stem (Rothwell, 2021), eustelic stem structure (Beck, 1970), and secondary growth from a bifacial vascular cambium (Beck, 1960). Most living gymnosperms also have axillary branching of the seed plant type (Rothwell, 1976; Stevenson, 2020). Evidence from previous studies reveals that many of these characters evolved in a non-synchronous fashion, with some being common to the most ancient gymnosperms (i.e., secondary vascular tissues from a bifacial vascular cambium; Hilton and Bateman 2006). Other characters apparently evolved later among ancient gymnosperms, including axillary branching, sympodial protoxylem architecture of the stem, eustelic stelar architecture of the stem, fully evolved stem-leaf organography, and indehiscent megasporangia and pollination (Seward, 1911; Galtier, 1977, 1999; Beck, 1970; Rothwell and Scheckler, 1988; Sanders et al., 2009; Stevenson, 2020; Stewart and Rothwell, 1993; Galtier and Meyer-Berthaud, 2006; Hilton and Bateman, 2006; Rothwell, 2021).

The evolution of still other characters has not yet been documented (i.e., cotyledonary embryo, bipolar growth) or else occurs in differing combinations among the most ancient gymnosperms, such that many of the characters we associate with modern gymnosperms appear to have evolved in a mosaic fashion among ancient extinct plants with gymnospermous biology. Against this background, the development of whole plant reconstructions and organismal concepts is crucial for documenting patterns of evolution for characters, and for resolving the pattern of phylogeny for the most ancient gymnosperms (Hilton and Bateman, 2009), most of which probably reproduced by hydrasperman reproduction.

The current study is a continuation of work begun more than 35 years ago with the goal of characterizing the plant community(s) represented by fossils preserved in and around the Oxroad Bay cliff assemblage (i.e., exposure A of Bateman and Rothwell, 1990, Bateman and Scott, 1990), and reconstructing plants that comprise those communities (Bateman and Rothwell, 1990). These goals are facilitated by unusual geology whereby fragments of whole plants are entombed in volcanic ash. Although substantial progress has been made toward those ends (Rothwell and Wight, 1989; Bateman and Rothwell, 1990; Rothwell and Scott, 1992; Dunn and Rothwell, 2012), *Tetrastichia bupatides* Gordon is the first detailed whole plant concept to be achieved for a gymnospermous plant species in the Oxroad Bay assemblages.

Herein we augment our understanding of the *Tetrastachia bupatides* plant by providing evidence for frond architecture, and structure of the distal frond and pinnules. We also document structure of the pollen producing organs, the identity and attachment of the ovulate cupules, and augment and evaluate the first direct evidence for rooting of a Devonian-

Mississippian hydrasperman seed fern. Although ovules have not yet been found in attachment to the *T. bupatides* plant, the Oxroad Bay material illuminates evidence for the nature of the seeds and allows us to offer a reconstruction characterizing the overall architecture and stature of the *Tetrastichia bupatides* plant (Fig. 1).

2. Materials and Methods

2.1. Material and occurrences

Plant fragments upon which the current study is based are preserved by calcareous cellular permineralization (sensu Schopf, 1975) in nearly a hundred in-situ and loose blocks from the cliff face (i.e., Exposure A of Bateman and Rothwell, 1990; Bateman and Scott, 1990) at Oxroad Bay, Tantallon, on the coast of East Lothian, Scotland (Plate I), and by siliceous cellular permineralization in blocks from the latest Devonian near Ballyheigue, County Kerry, Ireland. The Oxroad Bay material includes blocks, peels, and slides previously prepared and studied by Gordon (1938), Barnard (1959, 1960a, 1960b, 1962), Barnard and Long (1973), Long (1975), Rothwell and Scott (1985), Scott and Rex, (1987), Bateman (1988), Rothwell and Wight (1989), Bateman and Rothwell (1990), Bateman and Scott (1990), Scott (1990), and Dunn and Rothwell (2012; Table 1). A large percentage of the material from exposure A (Bateman and Scott, 1990) at Oxroad Bay, was collected in 1984 by R.M. Bateman, A.C. Scott, G.W. Rothwell and a contingent of workers from the Department of Geology, Chelsea College, University of London in 1984 (Bateman and Rothwell, 1990). The horizon and one of the calcareous cemented blocks of ash-bearing plants is from the same fossiliferous lens that was first sampled and described by Gordon (1938) and that yielded the

type material of *Tetrastichia bupatides* (Gordon, 1938; Plate I, 1-3).

Subsequent preparation of the material from the 1984 collection produced more than 8000 cellulose acetate peels (Joy et al., 1956), several hundred microscope slides of peels (Table 1) and ground thin sections (Stein et al., 1982 and references therein; Plate I, 5, 6). This Oxroad Bay material was studied in conjunction with the specimens published earlier by other workers (Gordon, 1938; Barnard, 1959, 1960a, 1960b; Barnard and Long, 1973; Long, 1975; Bateman and Rothwell, 1990, Dunn and Rothwell, 2012; Table 1). Thin sections were also prepared to study the preservation of the plant bearing ashes (Plate I: 4 – 6; Scott 1990).

Additional stems and rachides of *Tetrastichia bupatides* investigated in the current study are preserved in the flora of permineralized plant fragments in Late Devonian deposits near Ballyheigue, County Kerry on the west coast of southern Ireland (Matten et al., 1975, 1980a, 1980b, 1984; May and Matten, 1983). One of those specimens was initially recognized as *T. bupatides* (Matten et al., 1984). Others were described as *Laceya hibernica* May & Matten (May and Maten, 1983), but more recently recognized as falling within the range of variation for stems and frond bases of *T. bupatides* (Dunn and Rothwell, 2012). The Ballyheigue specimens include the most basal available stem segment with attached adventitious roots (Plate III, 7). They reveal that *T. bupatides* also occurs in uppermost Devonian deposits of southwestern Ireland, thus extending the geographic and stratigraphic ranges of the species and providing additional material for characterizing the plant.

2.2. Study techniques, preparation methods, and specimen repositories

Shoot morphologies, frond architecture, pinnule morphology, tap and adventitious root structure, pollen organ structure and attachment, and ovulate cupule structure and attachment

of *T. bupatides* are documented from serial sections of permineralized plant fragments prepared from blocks of largely calcareous matrix by the cellulose acetate peel technique (Joy et al., 1956). Peels are affixed to glass microscope slides with the xylene soluble mounting medium Eukitt (O. Kindler GmbH, Freiberg, Germany). Because most blocks also include opaque permineralizing minerals (e.g., pyrite), some specimens have been wafered into 1 mm thick sections using an Isomet slow speed saw (Buehler Corp., Lake Bluff, IL, USA) and mounted on microscope slides for study. Specimens preserved by siliceous cellular permineralization from the Ballyheigue, County Kerry on the west coast of southern Ireland were also serial sectioned by the cellulose acetate peel technique for previous studies (May and Matten 1983; Matten et al., 1984). Because histological features of this material are revealed in greatest detail while peels remain on the rock surfaces, most of the photographs of those sections were captured before the peels were removed.

Photo-microscopy was accomplished with an Olympus DP-12 digital camera mounted on Reichert Diastar and Olympus SZ-CTV microscopes, and a Nikon SMZ1500 Microscope with Digital Sight DS-2MBWc, DS-U1 Camera and NIS Freeware 2.10. Additional transmitted light images were captured using a Better Light digital scanning camera (Better Light Inc., Placerville, California, USA) mounted on a Leitz Aristophot large-format camera and focused through either Summar lenses or a Zeiss WL compound microscope. Images were processed and plates constructed using Adobe Photoshop CS3 Extended and stored as TIFF and PSD files. Identity and location of studied materials are detailed in Table 1. Images are archived at the Division of Paleobotany, Natural History Museum and Biodiversity Research Center, University of Kansas.

154 *2.3. Identification of plant fragments*

155 A close similarity of histological features among most small seed ferns preserved in
156 the Oxroad Bay cliff sediments (i.e., exposure A of Bateman and Rothwell 1990; Bateman
157 and Scott, 1990; Plate II, 2, 5) makes accurate identification and correlation of small frond
158 and other dispersed organ fragments extremely difficult. This has led to confusion about
159 identification of *Tetrastichia bupatides* and *Triradioxylon primaevum* Barnard & Long in
160 earlier studies (e.g., Pl. XI, Fig. 3 of Barnard, 1960a; Fig. 4e of Dunn and Rothwell, 2012).
161 However, there are several subtle differences in vascular tissue configurations and other
162 histological features between foliar fragments of *Tetrastichia bupatides* and those of
163 *Triradioxylon primaevum*, which are the most common vegetative gymnosperm fossils
164 preserved in Exposure A at Oxroad Bay (Bateman and Rothwell, 1990; Rothwell pers.
165 observations). Recent recognition of correlated combinations of such differences has allowed
166 for more accurate identification of most plant fragments (Table 2).

167 Pinnae of *Tetrastichia bupatides* have a variable number of small, more-or-less
168 interconnected bundles arranged in a row, a gentle arc, or a U-shape (Plate II, 1, 5 – 7; Plate
169 V, 3, 4). By contrast, those of *Triradioxylon* typically have one or two relatively large,
170 elliptical leaf traces (Plate II, 1, 5, at "Tri"). Whereas, both species have a well-developed
171 *Sparganum* Unger/*Dictyoxylon* Williamson-type sclerotic hypodermis and an inner
172 parenchymatous cortex, in *Triradioxylon* (Plate II, 1, 2, 5, at "Tri") the sclerotic zone is
173 relatively thicker than in *Tetrastichia* (Plate II, 1, 5, 7). Also, the individual sclerotic cortical
174 bundles of *Tetrastichia bupatides* (e.g., Plate II, 7) tend to be smaller and more widely spaced
175 than in *Triradioxylon primaevum*, which often has a nearly solid sclerotic outer cortex (Plate

176 II, 1, 2, 5). In *T. primaevum* the parenchyma cells of the inner cortex tend to have more robust
177 walls (i.e., often are more completely preserved) than those of *T. bupatides* and are more
178 tightly packed than in *T. bupatides*. In addition, some cells of the parenchymatous ground
179 tissue in *T. bupatides* have distinctive cells with black contents that typically are absent from
180 specimens of *T. primaevum* (Plate II). Together, these contrasting combinations of characters
181 (Table 2) aid in the confident identification of most tissue fragments in the permineralized
182 blocks from Exposure A at Oxroad Bay.
183
184 **3. Systematic Palaeobotany**
185 *Class*: SPERMATOPSIDA sensu Serbet and Rothwell, 1994
186 *Family*: TETRASTICHIACEAE Fam. Nov.
187 *Familial diagnosis*: Hydrasperman seed ferns with mesarch actinostele, narrow stelar ribs,
188 and sympodial protoxylem architecture. Fronds planar, forking proximally, pinnate distally;
189 rachial pinnules absent. Pollen organs attached to fronds distally; aggregate and compact,
190 consisting of cruciately forked, axes with inverted, round, simple synangia of elongated
191 sporangia attached to basal pad of tissue; prepollen trilete. Ovulate cupules large with ring of
192 highly dissected peripheral lobes surrounding numerous terete central lobes; attached at base
193 of fronds.
194 *Genus*: **Tetrastichia** Gordon 1938 emend.
195 *Type species: Tetrastichia bupatides* Gordon 1938
196 *Type Specimen (Letotype)*: In his original descripton of *Tetrastichia bupatides*, Gordon did
197 not designate a holotype specimen. Therefore, the 34 slides in the Gordon Collection, Natural

History Museum, GC: 1832, 1848, 1856, 1860-1862, 1872, 1878-1880, 1883, 1894, 1905, 1906, 1910, 1917, 1922, 1930, 1934, 1937, 1940-1942, 1949, 1951, 1962, 1968, 1971, 1984, 1987, 1998, 2001, 2003, 2006 have represented syntypes. Herein, we designate the first specimen figured by Gordon (Plate I, Fig. 2 of Gordon, 1938) as the Lectotype of *Tetrastichia bupatides* Gordon. This consists of Gordon slide No. 1861 and all other slides made from that specimen.

Localities: Lectotype and topotype specimens collected along North Sea coast, east of Tantallon Castle, East Lothian, Scotland, 40 km E of Edinburgh (NT599848), identified as Exposure A by Bateman and Rothwell (1990), and as documented by Bateman and Scott (1990; Plate I, 1-3). Additional specimens from exposure located adjacent to beach near Ballyeigue, Co. Kerry, Ireland (52^{o} 23’ 20” N; 9^{o} 50’ 30” W), as documented by May and Matten (1983).

Stratigraphy and Age:

Oxroad Bay Stratigraphy: The stratigraphic nomenclature of the Oxroad Bay sequence has been revised on several occasions since the publication of Bateman and Scott (1990) and Bateman et al. (1995). Currently the mixed succession of pyroclastic and reworked pyroclastic rocks in the cliff at Oxroad Bay belongs to the North Berwick Member, the basal unit of the Garleton Hills Volcanic Formation (Browne, et al., 1999; Monaghan and arrish 2006) that is stratigraphically above the Ballagan Formation.

Oxroad Bay Age: Two samples from 5 and 10 m below the position of the main Gordon plant bed yielded CM zone miospores that indicate a late Tournaisian age (i.e. Mississippian; Scott et al. 1984). These samples were reported to have been from localities B

and near exposure C of Bateman and Scott (1990). Bateman and Scott (1990) indicated that similar miospore assemblages occur in samples from Exposures D and E higher in the succession and this suggests that the entire plant-bearing sequence is of late Tournaisian age. The position of the CM and Pu zone boundary has proven controversial. In a borehole 9 km away, summarized graphically in the Dunbar memoir (Davies et al., 1986), more than 100 m of Pu zone Ballagan Formation are present beneath the base of the Garelton Hills Volcanic Formation. Note that volcaniclastic rocks are interbedded with the uppermost part of the Ballagan in the borehole and an abrupt conformable passage into the volcanic event is clear. It is not obvious, therefore, if the strata are of latest Tournaisian or earliest Visean in age (see Stephenson et al., 2004 for a discussion of some of the issues regarding the palynological zonation). The top of the Garleton Hills Volcanic pile has been radiometrically dated by Monaghan et al (2014) and the error bar extends to about 348 Ma. On the most recent International Chronostratigraphic Chart (https://stratigraphy.org/ICSchart/ChronostratChart2020-03.pdf) the Tournaisian-Visean boundary is now 346.7 ±0.4 Ma, so the Garleton Hills radiometric dates within error extend into the Tournaisian at least.

Ballyheigue Stratigraphy: The sequence belongs to the upper 200m of the Upper Old Red Sandstone. Stratigraphically the plant bed is located in the Inshaboy Formation (Diemer et al., 1987).

Ballyheigue Age: The age of the plant bed is dated by palynology. Miospore assemblages associated with the plant beds originally gave a Latest Devonian (LM Biozone) age to Bridge et al. (1980). Additional miospore assemblages studied by Higgs et al., (1988)

from the plant bed site gave a slightly younger Upper Devonian age. Higgs et al., (2013, p.35) assigned a LE Biozone age to the Plant Bed. The LE Biozone is Latest Famennian in age and palynological studies from well-dated marine sections in Germany show the LE miospore biozone is biostratigraphically constrained between the upper *expansa* to middle *praesulcata* conodont zones of Latest Famennian age (see Streel, 2009, p.172) (i.e., Devonian).

Emended combined generic and specific diagnosis: Upright plants having unbranched stem up to 22 mm in diameter, with determinant growth; fronds in 1/3, 2/5, or opposite/decussate phyllotaxy. Stem with three to five (possibly 6) narrow-ribbed protostele, most commonly four. Each rib with single mesarch, cauline protoxylem strand; intermittent central protoxylem infrequently present, but not contributing to frond vascularization. Secondary xylem in minority of stems, having numerous wide rays of all sizes. Cortex of inner parenchymatous zone with sclerotic clusters and cells with black contents; outer sclerotic zone of *Sparganum* and/or *Dictyoxylon*-type. Rachis trace initiation by radial division of single cauline protoxylem strand; more peripheral strand dividing tangentially, producing six-eight protoxylem strands located near abaxial margin of ribbed rachis trace. Diverging frond trace first forming 'butterfly' shaped bundle, ultimately appearing shallowly U-shaped. Rachis ≥10 cm long with pulvinus, typically forking twice to form tertiary rachides with opposite, subopposite, and alternate, highly dissected pinnules. Pinnules vascularized by terete trace with single protoxylem, originating from outer margin of corrugated tertiary rachis trace; pinnules forking repeatedly from base, with *Rhodea* Presl-type morphology. Roots of the *Amyelon* type, consisting of large branched taproot and small adventitious roots; typically

with tetrarch actinostele. Aggregate pollen organs, cruciately forked several times; terminating in simple synangia of six elongated sporangia. Cupules large and ellipsoidal, with structure conforming to *Calathospermum fimbriatum* Barnard; attached to base of rachis immediately distal to divergence of frond from stem.

4. Description of *Tetrastichia bupatides*

Earlier studies of *T. bupatides* provide detailed descriptions for the stems and frond bases (Gordon, 1938; Barnard, 1960a; May and Matten, 1983; Matten et al., 1984; Dunn and Rothwell, 2012), including ranges of variation for many features of external morphology, internal anatomy, phyllotaxis, and primary and secondary growth. Some evidence for rooting of the plant also has been introduced (May and Matten, 1983; Dunn and Rothwell, 2012), but not elaborated previously. These features (Gordon, 1938; Barnard, 1960a; May and Matten, 1983; Matten et al., 1984; Dunn and Rothwell, 2012) are summarized below; for details the reader is referred to the pertinent references.

4.1. Stem structure

Tetrastichia bupatides stems are narrow, ranging 8 – 22 mm in diameter. Among the specimens described by previous authors, stem branching has not been reported. Likewise, no evidence of stem branching has been found in our search for such among the large number of specimens available for study. Stems have a ribbed protostele with narrow ribs that vary in number from three to five or possibly six along the length of individual stem segments. Fronds are produced in 1/3, 2/5, and opposite/decussate arrangements depending on the structure of the stele at a given node. Internodal lengths are relatively short, ranging 5 to 42

286 mm, but incomplete internodes up to 9 cm also are present among the specimens. Stems have
287 a parenchymatous inner cortex with sclerotic nests and black contents in some cells, and a
288 sclerotic outer cortex that varies from the *Sparganum* to the *Dictyoxylon* configuration.
289 Secondary xylem is present in a small percentage of stems of all sizes, but primary cortex
290 remains intact even in those with the most wood (e.g., Plate III, 7). Therefore, stems did not
291 increase in girth due to the production of secondary tissues.

292 Stem protoxylem architecture is sympodial, with a cauline protoxylem strand located
293 midway along each stelar rib. A central protoxylem strand occurs intermittently in a few stems
294 but does not contribute to appendage vascularization. Vascularization of each frond begins
295 with the radial division of the sympodial protoxylem strand in a stelar rib. Proceeding distally,
296 the more peripheral protoxylem strand extends toward the tip of the rib and divides
297 tangentially to produce a row of up to about eight protoxylem strands near the abaxial surface
298 of one or a pair of metaxylem bundles. Frond divergence is at a wide angle (~80-90^0).

299 *4.2. Frond architecture and pinnule structure*

300 Because the fronds of *T. bupatides* are relatively large (up to ~0.3 m) and highly
301 dissected, there undoubtedly is variation among specimens. However, all vegetative divisions
302 are in the same plane (Table 3), forming a strictly planar frond. Together, information
303 developed in earlier studies (Gordon, 1938; Barnard, 1960a; Dunn and Rothwell, 2012) and
304 data gathered from several hundred foliar fragments (e.g., Plate II; Plate IV; Plate V, 1-5; e.g.,
305 Table 3) now provide evidence to characterize complete fronds. Fronds produce a distinct
306 pulvinus, and have a rachis that typically forks twice, the first 2 – 10 cm from the stem
307 (Gordon, 1938; Dunn and Rothwell, 2012). Rachial pinnules are absent, but two specimens

show the divergence of laterals with two protoxylem strands distal to the first fork (Table 3). The structure of those laterals is uncertain.

Branching of the tertiary pinnae is pinnate and variable, with opposite, subopposite, and alternate arrangements all represented among the frond fragments studied (e.g., Fig. 1g, 8b; Fig. 3 of Gordon, 1938; Figs. 15a, 15b, 15m-p of Barnard, 1960a; Figs. 8c-e of Dunn and Rothwell, 2012). Tertiary pinnae are roughly oval in cross sections, except at the levels of branching, where they have a concave adaxial surface (Plate II, 5, 7), and they produce only pinnules (e.g., Plate II, 7; IV, 1, 5). Individual tertiary pinnae range 1 – 3 mm wide (Table 3), with an arc- or c-shaped trace that consists of two to ~five more-or-less interconnected bundles (Plate II, 1, 5, 7; Plate IV, 2, 3; fig. 41 of Gordon, 1938), each with a single protoxylem strand near the abaxial surface of the metaxylem (e.g., Plate II, 7, at blue arrowheads). Vascular tissue is surrounded by mesophyll that consists of an inner zone of incompletely preserved parenchyma cells, some of which have black contents (Plate II, 7; Plate IV, 4) and outer zone of interconnected sclerenchyma bundles (Plate II, 1, 5, 7).

We found no evidence for the more highly dissected pinnate regions of the frond reconstructed by Barnard (i.e., Fig. 13 of Barnard, 1960a). Rather, tertiary pinnae produce laterals with the characteristic vascularization and structure of pinnules (Table 3). This occurs consistently by separation of one of the peripheral protoxylem strands and accompanying metaxylem from the pinna rachis bundle (Table 3; Plate IV, 5), followed by the divergence of an oval lateral member (Plate II, 7.) as the pinnule base. In an earlier study (Dunn and Rothwell, 2012) pinnule bases were identified by the lateral divergence of one bundle and surrounding tissues (e.g., Plate II, 7, at red arrowhead; Fig. 15 of Barnard, 1960a), but more

distal levels of the pinnules were not recognized.

Among the specimens available to the current study there are numerous attached and relatively complete pinnules sectioned in both cross (Plate II, 2-4, 8, 9; Plate IV, 5, 6) and longitudinal (Plate II, 5, 6) views. Attached pinnules are of the *Rhodea* type (sensu Arnold, 1947, Jennings, 1976), which is the most common morphology for pinnules of putative seed ferns from Mississippian (early Carboniferous) deposits up through Namurian A (e.g., Kidston, 1923; Arnold, 1947; Jennings, 1976; Scott, 1985; Rowe, 1988; Meyer-Berthaud, 1989; Taylor et al., 2009). Individual pinnules are roughly deltoid, ≥20 mm long (Plate II, 6) and ≥15 mm wide (Plate II, 2, 4).

Each pinnule consists of up to ~15-20 elongated narrow segments (Plate II, 5, 6) that fork dichotomously (Plate II, 3, 6) in a single plane (Plate II, 2, 4). The first dichotomy occurs immediately distal to the base of the pinnule (Plate II, 5, 7), and the number of forks varies among pinnules, with up to four successive forks occurring in a single section of an incomplete pinnule (Plate II, 6, at arrows). Between successive forks, each pinnule segment is oval in cross section (Plate II, 2, 4, 8), unless taphonomically distorted (Plate II, 9). Internally, pinnule segments have a single terete bundle surrounded by parenchymatous ground tissue in which a variable percentage of cells have black internal contents (Plate II, 2-9). A narrow zone of sclerotic cortex like that of the pinna rachis characterizes the diverging pinnule trace up to the level of the first fork (Plate II, 7, at center; Fig. 15O of Barnard, 1960a), but sclerenchyma is absent at more distal levels except between adjacent segments of branching lobes (Plate II, 3, 7, at arrows). There also is an inconspicuous uniseriate epidermis, but cells of that layer are typically not well preserved.

352 *4.3. Rooting of the plant*

353 Both a basal taproot system (Plate III, 1-5) and adventitious roots (Plate III, 6-8)
354 appear to be produced by stems of *T. bupatides*. One branching root, 4. 5 cm long, occurs in
355 attachment to a fragment with the characteristic cortical sclerenchyma of *T. bupatides* stems
356 (Plate III, 5, green arrowheads). The root apex (Plate III, 1) is incompletely preserved but
357 appears to be constructed of thin-walled cells (root cap and apical meristem?). Well-
358 developed secondary xylem is preserved within 4 mm of the root tip (Plate III, 2). This root is
359 tetrarch (Plate III, 4) with abundant secondary xylem and periderm (Plate III, 2-5), and
360 conforms to the genus *Amyelon* Williamson (Barnard, 1962). Branches are produced
361 endogenously (Plate III, 3, 5) within 7 mm of the root apex, and a total of 15 diverge
362 irregularly around the taproot to within 1 mm of the level attachment to the stem. All of the
363 branch roots are torn off 1-2 mm from the levels of divergence.

364 We consider this specimen to be a tap root system from which the stem has been
365 broken off just above the level to which the basal-most characteristic sclerenchyma cortical
366 pattern of *T. bupatides* extends (Plate III, 5). This interpretation is based on what we interpret
367 as cellular continuity between the most proximal level of the taproot and *Tetrastichia*-type
368 sclerotic cortex (Plate III, 5 at right). If correctly interpreted, the transition from stem to root
369 stelar structure in *T. bupatides* occurs above the level where the basal-most stem cortical
370 sclerenchyma ends, and this is why there is characteristic *T. bupatides* cortical sclerenchyma
371 at the uppermost preserved level of the branching root specimen (Plate III, 5).

372 Adventitious roots are produced by another stem specimen with abundant secondary
373 xylem (Plate III, 7), and that appears to be from a near basal level of the shoot. Diverging

roots are recognized as small steles among disrupted radial rows of secondary tracheids at the periphery of the stem stele (Plate III, 7, at red arrowheads) just distal to a diverging frond trace (within rectangle at upper left of Plate III, 7). These adventitious roots extend through and disrupt the cortex before emerging at the stem periphery (Plate III, 7 at R), beyond which all are broken off. At the level of emergence, the roots consist of a tetrarch protostele surrounded by a zone of parenchymatous cortex (Plate III, 8). In the specimen illustrated, three of the stelar ribs are longer than the fourth (Plate III, 8). Another specimen shows a woody root intersecting the stem and rachis base at the level of frond divergence (Plate III, 6), suggesting adventitious rooting at basal levels of the rachis. However, cellular continuity of the root and stem/frond juncture in this specimen is uncertain.

4.4. Pollen organ structure and attachment

Among the three morphotypes of putative seed fern pollen organs documented from Exposure A at Oxroad Bay (Bateman and Rothwell, 1990), an incomplete specimen of the large aggregate structure of the type designated “Pollen organ C” by Bateman and Rothwell (1990) forms the apical region of a *T. bupatides* pinna that also bears pinnules proximally (Plate IV, 1-6). Attachment of this pollen organ aggregate to a frond segment with the characters of a *T. bupatides* tertiary rachis is represented in a series of 230 serial sections. When photographs of 11 sections from this series are aligned and overlain, the composite photograph documents continuity of the vegetative and fertile regions of a specimen that is ~6 cm long (Plate IV, 1). This specimen consists of the apical region of what we interpret to be a tertiary pinna, the proximal 4 cm of which produces pinnules (Plate IV, 5, 6) in an alternate arrangement, and the distal two cm consists of an aggregate pollen organ (Plate IV, 7). The

vegetative region of the specimen has a trace with four protoxylem strands near the base of the pollen organ (Plate IV, 2, 3), parenchymatous mesophyll in which black cellular contents are common (Plate IV, 4), and weakly developed hypodermal sclerenchyma. The attached *Rhodea*-type pinnule bases (Plate IV, 5, 6) have the same structure as those described earlier (c.f., Plate II, 5 and Plate IV, 5, 6; Dunn and Rothwell, 2012).

The overall architecture of the aggregate pollen organ is difficult to determine from this specimen alone, because it apparently is incomplete. However, like more complete specimens described by previous workers (e.g., Fig. 1j of Bateman and Rothwell, 1990), this specimen displays closely spaced, relatively equal cruciate dichotomies basally, and then unequal, cruciate dichotomies (Plate IV, 8). Each of the unequal dichotomies produces a smaller unit that terminates in a simple pollen organ (Plate IV, 9) and a larger unit that continues to fork unequally, producing additional simple synangia. The ultimate segments are inverted with respect to the larger unit from which they are produced (Plate IV, 9), and terminate in an expanded cushion (Plate IV, 9, 10, 13, at c) that bears a ring of elongated sporangia that are not laterally confluent (Plate IV, 7, 9-11, 13, 14). The number of sporangia per simple synangium is difficult to determine because such synangia are closely spaced, oriented at different angles, often distorted (Plate IV, 7, 9, 10, 13), and the individual sporangia are not fused to each other distal to the basal cushion (Plate IV, 9-11, 13). Nevertheless, where individual synangia can be identified, each has six sporangia (e.g., Plate IV, 9, 11). Sporangia have an epidermis of small rectangular cells (Plate IV, 14 at arrow), and one to two layers of inner wall cells with black contents (Plate IV, 14). Dehiscence is via a longitudinal slit that occurs toward the center of the synangium, where the inner cell layers

418 appear to be absent.

419 Prepollen within this type of synangium (i.e., Figs. 4g and 9k of Bateman and
420 Rothwell, 1990) has been figured earlier as consisting of radial, trilete grains with a bimodal
421 range of size distribution (i.e., ~100 μm, and 25-50 μm in diameter). The exine of prepollen
422 from the larger cohort is finely granulate (Bateman and Rothwell, 1990). We note the
423 common occurrence of similar prepollen grains in other apparently hydrasperman Paleozoic
424 pteridosperm pollen organs (Meyer-Berthaud, 1989). The aggregate synangial clusters,
425 interior forking segments, and simple synangia are all immersed in a cloud of trichomes (Plate
426 IV, 12) that curve such that only short segments appear in longitudinal views (Plate IV, 12, at
427 red arrowhead). In cross sections the trichomes are approximately 80 μm in diameter.

428 *4.5. Cupule structure and attachment*

429 As previously suspected, ovulate cupules of *T. bupatides* conform to *Calathospermum*
430 *fimbriatum* (1960b), the detailed structure of which has been described thoroughly in previous
431 studies (Barnard, 1960b; Long, 1975). The specimen presented on Plate V, 1-11, has a cupule
432 stalk that is more or less round in cross section, with a U-shaped trace that has seven
433 protoxylem strands (Plate V, 6), and inner and outer cortex like those of *T. bupatides* rachides
434 (Plate V, 3-5). About 5 mm from the base of the cupule stalk, tissue extends away from the
435 surface of the stalk (Plate V, 3) as do basal laterals previously described for *C. fimbriatum*
436 (Barnard, 1960b). Progressing distally, the stalk first undergoes a series of cruciate forks, and
437 then the cupule lobes undergo both cruciate divisions and divisions in the same plane (Plate
438 V, 1, 2). Repeated divisions of both types produce a roughly ellipsoidal cupule consisting of a
439 ring of narrow exterior vegetative segments (Plate V, 10, 11) and numerous terete segments to

the interior (Plate V, 10). In all of these characters, this cupule conforms to previously described specimens of *C. fimbriatum* from Exposure A at Oxroad Bay (Barnard, 1960b; Long, 1975; Bateman and Rothwell, 1990).

Ovulate cupule identity as an organ of the *T. bupatides* plant is established by a series of sections in which the *C. fimbriatum* cupule stalk is attached to the base of a *T. bupatides* frond immediately distal to frond divergence from the stem (Plate V, 1-9). The attached frond and cupule are both bent backward toward the base of the stem (Plate V, 1-4), presumably as the result of taphonomic distortion within the pyroclastic mudflow. The cupule is largely torn away from the juncture of the stem and frond (Plate V, 5, 7). However, it does retain cellular continuity along a narrow zone of ground tissue (Plate V, 8, 9).

Progressing basipetally from the node, sections show divergence of the frond and cupule at about the same level (Plate V, 4, 5), with the cupule (Plate V, 5, 7-9) being slightly more proximal than the rachis (Plate V, 5). Using a rib of the stem protostele as a gauge (blue lines on Plate V, 5), the cupule stalk is oriented (diagonal blue line on Plate V, 5) at about 35-40% from the radius upon which the frond diverges (vertical blue line on Plate V, 5). In contrast to the cupule, continuity of the stem and frond is well represented by both vascular and ground tissues. Attachment of the cupule to the frond base, rather than to the stem is inferred from the absence of any vascular tissue in the stem other than the frond trace diverging from the stem stele at that node (Plate V, 4, 5). Organic attachment of the cupule is documented by a series of sections through the node in which stem tissue extends radially toward the cupule stalk (Plate V, 4, 5 at arrow, 7), the two organs becoming increasingly closely spaced until a narrow bridge of ground tissue (Plate V, 8) attaches the two organs

462 (Plate V, 9). We interpret this cupule to have been nearly completely torn away from the frond
463 base, leaving only the narrowest of tissue continuity to document the attachment.
464
465 **5. Discussion**
466 Bateman and Rothwell (1990) outlined, and Hilton and Bateman (2009) further
467 elaborated some of the evidence and concepts commonly applied to whole plant
468 reconstructions of extinct species, including, 1) organic connection of organs, 2)
469 morphological and/or anatomical similarities, 3) association/disassociation of organs in the
470 same matrix, 4) conceptual models including previously reconstructed fossil plants and
471 articulated modern analogues, and 5) ontogeny. Despite apparently having been ripped up,
472 transported, and deposited in volcanoclastic mud flows (Rothwell and Scott, 1985; Bateman,
473 1988; Bateman and Scott, 1990), the Oxroad Bay fossils of *T. bupatides* include an extremely
474 large number (>1,000) of well preserved, permineralized plant fragments. These include 1) an
475 interconnected stem, frond base, and ovulate cupule, 2) several interconnected stems, frond
476 bases, and/or roots, 3) frond fragments with overlapping ranges of variation, and 4)
477 interconnected pinnae, pinnules, and an aggregate pollen organ, provide unequivocal evidence
478 for nearly all the vegetative and fertile organs of the *Tetrastachia bupatides* plant. This
479 information has been incorporated into a suggested reconstruction of a single plant (Fig. 1).
480 As elaborated below, only the identity of the ovules remains in question for *T. bupatides*.
481 *5.1. Summary of organ structure for the Tetrastichia bupatides plant*
482 The stems of *T. bupatides* are narrow and unbranched, ranging 8 – 22 mm in diameter
483 (Fig. 1), with a protostele of 3 to 5 (or 6?) narrow xylem ribs, and sympodial protoxylem

484 architecture. Fronds are produced in 1/3, 2/5, and opposite/decussate arrangements, which
485 may change from level to level of the same stem. Most stems have little or no secondary
486 tissue, but significant wood surrounds the stele and accompanies diverging frond traces in a
487 minority of specimens.

488 Fronds have a prominent pulvinus and branch in a single plane to form a foliar organ
489 that is flattened in its vegetative regions. There undoubtedly is variation in frond structure
490 along the length of the stem, as has been documented previously for the seed fern
491 *Calathopteris heterophylla* Long from Oxroad Bay (Long, 1976). The rachis of relatively
492 large fronds (Fig. 1) typically forks 2 – 10 cm from the stem, and a second time to produce
493 four tertiary pinnae (Dunn and Rothwell, 2012; Fig. 1). Rachial pinnules are absent. Tertiary
494 pinnae produce highly dissected pinnules in a combination of alternate, subopposite, and
495 opposite arrangements (Table 3). Pinnules are of the *Rhodea* type, which is the most common
496 putative seed fern pinnule morphology in early Carboniferous (Mississippian) deposits (e.g.,
497 Kidston, 1923; Jennings, 1976; Scott, 1985; Plate. II). Among the compression specimens of
498 frond fragments described from the Oxroad Bay localities, we consider the morphology of *T.*
499 *bupatides* pinnules to be most similar to those in Fig. 7a (from Exposure F) of Bateman and
500 Rothwell (1990).

501 5.2. *Features of the Tetrastichia bupatides plant*

502 The *T. bupatides* plant appears to have been rooted by a basal, branching taproot, and
503 also by adventitious roots that diverge near the base of the stem (Fig. 1). If this information is
504 accurate, then the plant probably has bipolar growth, possibly from a cotyledonary embryo.
505 The origins of both cotyledonary embryos and of bipolar growth among the most ancient

506 gymnosperms have not been established previously, and only indirect evidence is provided by
507 the *T. bupatides* fossils. Nevertheless, available data positively correlate with the earlier
508 description of an isolated structure interpreted to be a cotyledonary embryo from roughly
509 coeval deposits along the River Whiteadder in the Scottish borders (Long, 1975; Scott et al.,
510 1984). That longitudinally sectioned specimen is vascularized, with an apparent root cap at
511 one end and two cotyledon-like structures at the other (Figs. 58-65 of Long, 1975). The
512 absence of a nucellus and integument surrounding the putative embryo at the preserved stage
513 of development is unexpected. Therefore, the identity of the specimen as an embryo was
514 proposed with caution (Long, 1975). However, if correctly interpreted, that specimen does
515 establish that cotyledonary embryos and the correlated bipolar growth of seed plants
516 (Rothwell et al., 2014) originated by at least as early as the base of the Carboniferous. It also
517 increases the probability that our interpretation of a taproot for *T. bupatides* (Plate II, 1-5) may
518 be accurate.

519 Fronds of *T. bupatides* bear aggregate-type pollen organs terminally on tertiary pinnae
520 (Plate. IV, 1; Fig. 1). The pollen organ aggregates are compact, branched by closely spaced
521 cruciate dichotomies, and bear round simple, inverted synangia of typically six unfused
522 sporangia on a terminal pad (Plate IV). Sporangia dehisce via a longitudinal slit located
523 toward the center of the simple synangia (Plate IV, 7, 9, 11), and prepollen is radial and
524 trilete, with a finely granulate exine (Bateman and Rothwell, 1990). Among the four
525 morphological types of Early Mississippian fertile branched fronds characterized by Meyer-
526 Berthaud (1989), those of *T. bupatides* are most similar to “Type C”. However, the rachis of
527 *T. bupatides* forks twice (rather than once), and it bears simple synangia that form tight

528 aggregates on distal frond segments (rather than occurring in the positions of vegetative
529 pinnules (see Text-fig. 2 of Meyer-Berthaud, 1989).

530 Ovulate cupules of *T. bupatides* are of the *Calathospermum fimbriatum*-type (Plate V,
531 1, 10), and are attached at the base of the frond (Plate V, 5, 7-9) by a cylindrical stalk with a
532 C-shaped bundle (Plate V, 3-6) that closely resembles that of the frond rachis (Gordon, 1938;
533 Dunn and Rothwell, 2012). Such cupules are large, highly dissected, radial structures (Plate
534 V, 1, 10) with oppositely-arranged basal pinnules, peripheral vegetative lobes that encircle a
535 central area (Barnard, 1960b), and numerous small, terete internal lobes (Plate V, 10; Barnard,
536 1960b; Long, 1975) that are each thought to terminate in a single ovule (Barnard, 1960a;
537 Long, 1975). Although ovules do occur within with in *C. fimbriatum* cupules in Exposure A at
538 Oxroad Bay (e.g., Plate V, 10, 11; Barnard, 1960b), such ovules are assignable to several
539 species (e.g., Plate V. 10, 11), none has been documented as attached to a cupule lobe, and all
540 probably have been washed into the cupule interiors.

541 Barnard (1960b) described and illustrated a radial ovule in one *C. fimbriatum* cupule
542 that he identified as an immature specimen of *Salpingostoma dasu* Gordon. However, that
543 specimen conforms more closely to *Tantallosperma setigera* Barnard and Long (Bateman and
544 Rothwell, 1990), a species that was subsequently described from the same exposure (Barnard
545 and Long, 1973). One *Callathospermum* type cupule collected along the River Whiteadder
546 between Edrom and West Blanerne and assigned to *C. fimbriatum* does have attached ovules
547 that have been identified as *S. dasu* (Long, 1975). That cupule bears 12 attached, radial ovules
548 that apparently are in varying stages of maturity (Long, 1975). The ovules appear to have six
549 lobes, and are covered by a ramentum of trichomes, characters that are all shared with

specimens of *S. dasu* (Gordon, 1941; Long, 1975). However, those characters also are shared by another ovule from the same exposure, *Dolichosperma hexangulata* Long, which is apparently much more common at localities along the River Whiteadder than is *S. dasu* (Long, 1975).

Whereas mid-regions of attached ovules measured from Figures 39 and 40 of Long (1975) range 1.1 - 1.7 mm in diameter, dispersed ovules of *D. hexangulata* range 1.75 – 2.03 mm in diameter (Table 4 of Long, 1975) and dispersed ovules of *S. dasu* measure 5.0 – 6.6 mm in diameter (Gordon, 1941). Attached ovules are not well enough preserved to display finer features of structure that could help establish which, if either, of these species they represent (Long, 1975). General similarities between *D. hexangulata* and *S. dasu* that make identification of incompletely preserved, immature specimens difficult to establish include ovule symmetry, integument of highly dissected lobes, numbers of lobes, and the dense covering of trichomes. Therefore, because of the much closer size ranges of the *C. fimbriatum* ovules to those of *D. hexangulata* than to *S. dasu* (Long, 1975), it appears that the identity of the *C. fimbriatum* ovules discovered by Long (1975) is less certain than originally thought. Indeed, because *D. hexangulata* appears to be more common at localities along the River Whiteadder than are specimens of *S. dasu*, *D. hexangulata* may be a more attractive candidate for the ovules of the *Calathospermum* cupule from the River Whiteadder localities than is *S. dasu*.

Dispersed ovules of *D. hexangulata* have not been identified from Exposure A at Oxroad Bay. Therefore, it is unlikely that ovules borne in *C. fimbriatum* cupules at Oxroad Bay are assignable to *D. hexangulata*. Likewise, because we now realize that *S. dasu* ovules

have not been found in attachment to *Calathospermum* cupules at Oxroad Bay, the identity of *T. bupatides* ovules remains in question. Indeed, another species of ovules from Exposure A at Oxroad Bay actually may have been part of the *T. bupatides* plant. The most common species of dispersed ovules present at Exposure A at Oxroad Bay is the flattened species *Eosperma oxroadense* Barnard (Rothwell personal observations). *Eosperma oxroadense* is also the most common dispersed ovule present in (but not attached to) the *C. fimbriatum* cupule in attachment to the *T. bupatides* shoot (Plate V, 10, 11).

Although most *E. oxroadense* specimens are detached at the base of the ovule, a few remain attached to the apex of a terete axis that may be branched at a more proximal level (Barnard, 1959). One such *E. oxroadense* ovule studied in the current investigation is sectioned in near mid-longitudinal view of the minor plane of symmetry (Plate V, 12). When illustrated at the same magnification as a cross section of one of the internal cupule lobes of *C. fimbriatum*, the close resemblance of the *E. oxroadense* stalk to the internal lobe of *C. fimbriatum* is striking (c.f., Plate V, 13 and 14). Both are oval in cross section, ~1.0 – 1.8 mm in diameter. Each has an outer zone of prominent cells with incompletely preserved walls, a broad inner zone of cells with poorly preserved thin walls, and a terete bundle of several small tracheids (Plate V, 13 and 14, at arrowheads). Also, some cells near the periphery of each have black contents like those that characterize the ground tissues of *T. bupatides*.

We note that the largest prepollen grains produced by the type of aggregate pollen organs that have been found in attachment to *T. bupatides* fronds are larger than the diameter of the micropylar canal in *E. oxroadense*, which may reduce the probability that *E. oxroadense* represents the ovule of T. bupatides. However, we also note that the biological

implications of the bimodal distribution of grain size in the sporangia of *T. bupatides* are not understood. As a result, we stress that identity of the ovules produced by *Tetrastichia bupatides* remains equivocal, but available data suggest that *Eosperma oxroadense* is at least as attractive a candidate as is *Salpingostoma dasu.*

5.3. Tetrastichia bupatides as a hydrdasperman gymnosperm

Hydrasperman seed ferns are a reproductive grade of gymnosperms characterized by ovule structure and development, and by a distinctive mode of pollination and post-pollination biology (Rothwell, 1971, 1986; Niklas, 1983, 1985; Serbet and Rothwell, 1995; Hilton and Bateman, 2006; Scott et al., 2019). They make up the earliest well understood evidence for seed plants from the fossil record, extending from the Late Devonian through the Permian, and based upon the stratigraphic distribution of Paleozoic ovule morphologies (Seward, 1911), they are the only well-known gymnosperms that have been documented from the strata from which *T. bupatides* specimens have been recovered. Plants with hydrasperman reproduction produce a range of growth architectures. These range from small shrubs, to vines, to large trees (Galtier, 1988; Galtier and Scott, 1994), but all apparently produced highly dissected, fern-like leaves (e.g., *Pitys*, Long, 1963; Galtier, 1974) upon which reproductive structures were borne in separate pollen organs and ovulate cupules (Stewart and Rothwell, 1993; Meyer-Berthaud, 1989; Taylor et al., 2009).

Stems of hydrasperman seed ferns vary from those with a central cauline protoxylem strand at the center of an actinostele with narrow arms (e.g., *Triradioxylon primaevum*, Barnard and Long, 1975; *Elkinsia polymorpha* Rothwell, Scheckler & Gillesipe, Serbet and Rothwell, 1992), to actinostelic forms with sympodial protoxylem architecture (e.g., *T.*

616 *bupatides*), to those with round protosteles with a ring of peripheral protoxylem strands (e.g.,
617 *Heterangium* Corda, Hirmer, 1933), to those with an intergrading range of metaxylem
618 dissection leading to the eustele (e.g., *Lyginopteris* Potonié, Blanc-Louvel, 1966; Beck, 1970;
619 reviewed by Beck et al., 1982 and Galtier, 1988; Dunn, 2006). As with other hydraspermans
620 from Late Devonian and basal Mississippian deposits, *T. primaevum* lies near one end of that
621 range of variation, presumably displaying most of the plesiomorphic stelar characters of
622 gymnosperms (Galtier, 1988; Serbet and Rothwell, 1992).

623 Hydrasperman fronds typically fork at least once at the base, and most often branch in
624 a pinnate fashion distally (e.g., Blanc-Louvel, 1966; Rothwell and Taylor, 1972; Galtier,
625 1974; Jennings, 1976; Meyer-Berthaud, 1989; Taylor et al., 2009). Such fronds produce
626 pinnules that range from lobed forms often assigned to *Sphenopteris* (Brongniart) Sternberg or
627 *Mariopteris* Zeiller (e.g., Seward, 1911; Stidd and Phillips, 1973), to highly dissected forms
628 such as *Rhodea* (e.g., Lindley and Hutton, 1831; Kidston, 1923; Danźe-Corsin, 1953;
629 Jennings, 1976; Galtier, 1981) that are most common in Mississippian and Pennsylvanian
630 deposits (Kidston, 1923). With a twice-forked rachis and *Rhodea*-type pinnules borne on the
631 tertiary rachides (Fig. 1), *T. bupatides* fronds fall within the range of variation that is
632 characteristic of Mississippian (early Carboniferous) hydrasperman seed ferns.

633 Microsporangiate structures of the most ancient gymnosperms (reviewed by Millay
634 and Taylor, 1979, and Meyer-Berthaud, 1989) typically consist of a ring (or paired rows) of
635 sporangia that most often either are attached to an expanded pad of tissue or else are laterally
636 confluent for varying distances toward the apex of the sporangia (Meyer-Berthaud, 1989).
637 Some of these simple synangia are interspersed with pinnules on distal regions of the frond

638 (e.g., Jennings, 1976). Others, like those of the *T. bupatides* plant, consist of aggregates of
639 simple synangia. Still others form clusters of simple synangia that are fused together to form a
640 compound synangium (Millay and Taylor, 1979; Meyer-Berthaud, 1989). The elongated
641 sporangia of such fructifications dehisce via a longitudinal slit located toward the center of the
642 simple synangium, and typically produce radial, trilete prepollen grains (Millay and Taylor,
643 1979; Meyer-Berthaud, 1989). In all these respects, *T. bupatides* conforms to what is expected
644 for a hydrasperman seed fern.

645 Likewise, hydrasperman ovules are typically borne on fronds within specialized
646 structures termed cupules that facilitate pollination (Niklas, 1983) and probably also provide
647 protection for the developing ovules. Cupules may contain a single ovule (e.g., on the
648 *Lyginopteris oldhamia* plant; Oliver and Scott, 1904) or be multi-ovulate (e.g.,
649 *Genomosperma kidstoni* Long, Meade et al., 2021; *Diplopteridium holdenii* Lele & Walton,
650 Rowe, 1988; *Pollaritheca longii* Rothwell & Wight, 1989; *Elkinsia polymorpha* Rothwell,
651 Scheckler & Gilespie, Serbet &Rothwell, 1992; *Kerryia mattenii* Rothwell & Wight, 1989;
652 *Gnetopsis elliptica* Renault & Zeiller, Galtier, 2013). Cupules are borne on fronds either
653 terminally (e.g., *Elkinsia polymorpha*; Serbet and Rothwell, 1992; *Tristichia ovensii* Long,
654 1961), among pinnules in the distal regions of the frond (e.g., on the *Lyginopteris oldhamia*
655 plant, Seward, 1911), or in clusters that are attached at the level of the basal "fork" of the
656 frond (e.g., *Diplopteridium holdenii* Rowe, 1988). The attachment of *Calathospermum*
657 *fimbriatum* cupules at the base of the frond (Fig. 1), demonstrates yet another variation in
658 cupule position on the fronds of hydrasperman plants.

659 *5.4. Plant reconstruction*

660 Previous reconstructions of the growth architecture of Paleozoic seed ferns include
661 small trees or shrubs large trees (e.g., Long, 1979; Retallack and Dilcher, 1988; Speck and
662 Rowe, 1994; Zodrow et al., 2007), small scrambling, climbing, or leaning plants (Baxter,
663 1949; Pfefferkorn et al., 1984; Hamer and Rothwell, 1988; Krings and Kerp, 1999; Galtier
664 and Béthoux, 2002; Dunn et al. 2003). By contrast, the unbranched shoots of *T. bupatides*
665 have small stems (up to only ~ 2 cm), and short internodal lengths (i.e., ~ 5 – 90 mm) and
666 there is no evidence of spines, hooks, or other specializations of *T. bupatides* organs that
667 characterize Paleozoic seed fern vines (e.g., *Callistophyton boyssetii* (Renault) Rothwell,
668 1975; *Blanzyopteris praedentata* (Gothan) Krings & Kerp, 1999). Therefore, it is unlikely that
669 *Tetrastichia* was either a tree or a vine.
670 All *T. bupatides* stems are narrow (~28– 22 mm) and radial, with a ribbed protostele
671 and well developed *Sparganum/Dictyoxylon* type outer cortex. Oppositely and alternately
672 arranged fronds diverge from relatively closely spaced nodes (i.e., ~5 – 90 mm) all around the
673 radial stem (Fig. 1). The specimen with the greatest amount to secondary xylem (e.g., Plate
674 III, 7) produces adventitious roots (Plate I, 7, 8) suggesting it is a near-basal level of a stem.
675 Most stems have no secondary tissues (Dunn and Rothwell 2012), and our search among the
676 large number of stem fragments available for study has yielded no evidence of branching.
677 Because all of the smallest stems have no secondary tissues, they appear to be from distal
678 regions of the shoot, where they represent a level of apoxogenesis (i.e., diminishing growth
679 sensu Eggert, 1961; Masselter et al., 2007). Together with these features, adventitious roots at
680 basal levels of the stem, and evidence for a basal taproot suggest that individual genets were
681 small upright plants (Fig. 1). The Upper Devonian hydrasperman gymnosperm *Elkinsia*

682 *polymorpha* Rothwell, Scheckler & Gillespie also has bee n reconstructed as a small,
683 unbranched, upright plant (Serbet and Rothwell, 1992), but no stems of E. *polymoprha* with
684 attached roots have been discovered to date.

685 Vegetative fronds of *T. bupatides* are planar, all branches occurring in the same plane
686 (Fig. 1). They have a basal pulvinus, a rachis that forks twice into four pinnate units, each of
687 which bears highly dissected pinnules of the *Rhodea* type in both opposite and alternate
688 arrangements (Fig. 1). Aggregate pollen organs are borne at the tip of some of the pinnate
689 unites, and large *Calathospermum* type seed cupules are attached at the side of the frond base
690 (Fig. 1). Stems are surprisingly narrow for a plant that has large fronds ~30 cm long with large
691 aggretate pollen organs ~4 cm in greatest dimension and large seed cupules more than 2 cm in
692 diameter. Therefore, the narrow stems must have been stiffened by the outer
693 sclerenchymatous cortex, as has been demonstrated for some other hydrasperman seed ferns
694 with narrow stems (e.g., *Schopfiastrum decussatum* Andrews, Rothwell & Taylor, 1972;
695 *Lygniopteris oldhamia* (Binney) Potonié, Masselter et al., 2007). Although *L. oldhamia* and
696 other species of the genus are known to be lianas (e.g., *L royalii* Tomescu, Rothwell &
697 Mapes; Tomescu et al., 2001), *L. oldhamia* is interpreted to have a juvenile stage of growth in
698 which the sclerotic outer cortex provided sufficient stiffness for the stem to stand upright
699 (Masselter et al., 2007). We interpret the stem of *T. bupatides* to have been held upright by the
700 combination of several features. The architectural properties of the outer sclerotic cortex
701 would have contributed significantly to stiffening the stem and basal fronds may have bent
702 downward to contact the ground (Fig. 1). Moreover, *T. bupatides* plants could have grown in
703 closely spaced stands, providing mutual support for adjacent plants.

Adventitious prop roots (from frond bases?) would have provided additional support. Such roots were produced in the axils of leaf traces (Plate I, 6) at basal levels of the stem, and possibly also on fronds below the first fork (Plate I, 7) and just below the second fork (Gordon, 1938; Fig 7-C of Dunn and Rothwell, 2012). The occurrence of adventitious roots near the base of fronds would account for divergence of vascular bundles of otherwise unknown identity from one specimen from Oxroad Bay (Gordon, 1938;) and another plant from Ballyheigue (i.e., Fig. 28 of May and Matten, 1983).

5.5. Systematic relationships of Tetrastichia bupatides

All well characterized seed ferns from Mississippian strata and all the ovules present at Oxroad Bay (Bateman and Rothwell,1990) are of the hydrasperman type. Therefore, we interpret *T. bupatides* to hydrasperman as well. However, beyond that general systematic placement, more detailed relationships of *T. bupatides* are far less certain. *Tetrastichia bupatides* is often placed among the lyginopterid seed ferns (e.g., Dunn and Rothwell, 2012), itself a paraphyletic or polyphyletic assemblage (Taylor, et al., 2009), and a group defined by several highly variable characters (Galtier, 1988; Stewart and Rothwell, 1993). The clearest synapomorphy for the group is probably hydrasperman reproduction (Rothwell, 1986). There are wide ranges of variation among the plant architectures, stem structures (e.g., Galtier, 1988), stem branching (Galtier, 1982), frond morphologies (e.g., Kidston, 1923), pollen organ morphologies (e.g., Millay and Taylor, 1979; Meyer-Berthaud, 1989), ovule morphologies (e.g., Long, 1975; Scott et al., 2019), ovulate cupule morphologies (Taylor et al., 2009), and the placement of fertile structures on hydrasperman seed fern fronds (e.g., Meyer-Berthaud, 1989).

Only a tiny fraction of potential whole plant concepts have been developed for the most ancient seed plants. Therefore, it is not surprising that a widely accepted formal hierarchical classification has not yet been developed for hydrasperman gymnosperms. Given the current level of understanding of the "whole plants" that constitute hydrasperman gymnosperms, we consider this to accurately reflect what we understand at this time.

5.6. Evolutionary environment of the plants

The Ballyheigue specimens are preserved in Facies Association 2 of Bridge et al (1980). This facies association is characterised by sandstone-mudstone inter-beds (olive grey, yellow, green and red colours). The depositional environment has been interpreted as seasonal flood deposits associated with crevasse channels and splays, levees on vegetated floodplains. It is likely, therefore, that *Tetrastichia* lived in a disturbed environmental setting. Recent research has indicated that there was a major ecosystem disruption, termed the Hangenberg Event or crisis (Becker, Kaiser and Aretz, 2016; Kaiser et al., 2016). During this interval in the latest Devonian numerous plants and animals became extinct (Caplan and Bustin, 1999; Silvestro et al., 2015; Prestianni et al., 2016) and in addition marine systems were disrupted (Marshall et al., 2020). Evidently, *Tetrastichia* survived this perturbation and it may be significant that it is found in the Mississippian in the highly disturbed volcanic environment as seen in Oxroad Bay. These volcanogenic sediments were probably found associated with tuff ring volcanism and are found in a mixture of primarily deposited ashes as well as in volcanic mudflows or lahahs (Bateman and Scott, 1990; Scott, 1990; Bateman et al., 1995). Some of the features of the *Tetrastichia* plant, therefore, may have helped it survive a range of environmental trauma.

748

749 **Declaration of Competing Interest**

750 The authors certify that they have no affiliations with or involvement in any
751 organization or entity with any financial interest (such as honoraria; educational grants;
752 participation in speakers' bureaus; membership, employment, consultancies, stock ownership,
753 or other equity interest; and expert testimony or patent-licensing arrangements), or non-
754 financial interest (such as personal or professional relationships, affiliations, knowledge or
755 beliefs) in the subject matter or materials discussed in this manuscript.

756

757 **Acknowledgements**

758 The authors cheerfully dedicate this work to our valued colleague, Jean Galtier, who's
759 insightful contributions to fern and gymnosperm paleobotany have dramatically enhanced the
760 understanding of Mississippian-Pennsylvanian vegetation, and particularly for his more than
761 50 years of enduring friendship and support. The Department of Geology, Chelsea College of
762 the University of London is acknowledged for hosting the senior author while on sabbatical
763 leave to initiate this project in 1984. We also are grateful for collecting assistance provided by
764 the staff and students of the same department, particularly Richard Bateman, Steve Brindley,
765 Keith Stephens and Kate Bartram. Cedric Shute and Peta Hayes graciously provided access to
766 collection materials of the Natural History Museum, London, and Rudy Serbet provided
767 access to the Oxroad Bay material housed at the Museum of Paleontology, University of
768 Kansas. Gene Mapes (Ohio University) contributed helpful discussions, and Ruth Stockey
769 (Oregon State University) aided in editing the manuscript. The *Tetrastichia bupatides* plant

770 reconstruction in Fig. 1 was rendered by Lynne Blything. We thank Alison Monaghan and
771 David Millward for discussion concerning the stratigraphy and dating of Oxroad Bay, Ken
772 Higgs for discussion of the Ballyheigue site, and Jason Hilton and an anonymous reviewer for
773 helpful comments and recommendations for modifications to the manuscript. This work was
774 supported by the National Science Foundation (grants No. BSR86-00660 and DEB-9527920
775 to G.W.R.) and a grant from NERC (GR3/4986) to A.C.S.

776

Literature Cited

Arnold, C.A., 1947. Paleobotany. McGraw-Hill Book Co. 433 pp.

Barnard, P.D.W., 1959. On *Eosperma oxroadense* gen. et sp. nov.; a new Lower Carboniferous seed from East Lothian. Ann Bot (NS) 23: 285-296.

Barnard, P.D.W., 1960a. Studies on some Lower Carboniferous plants from East Lothian. PhD thesis. London University. 290 pp.

Barnard, P.D.W., 1960b. *Calathospermum fimbriatum* sp. nov., a Lower Carboniferous pteridosperm cupule from Scotland. Palaeontol 3: 265-275.

Barnard, P.D.W., 1962. Revision of the genus *Amyelon* Williamson. Palaeontol 5:213–224.

Barnard, P.D.W., Long, A.B., 1973. On the structure of a petrified stem and some associated seeds from the Lower Carboniferous rocks of East Lothian, Scotland. Trans R Soc Edinb 69:91-108.

Barnard, P.D.W., Long, A.B., 1975. *Triradioxylon*—a new genus of Lower Carboniferous petrified stems and petioles together with a review of the classification of early Pterophytina. Trans R Soc Edinb 69:231-250.

Bateman, R.M., 1988. Palaeobotany and palaeoenvironments of Lower Carboniferous floras from two volcanigenic terrains in the Scottish Midland Valley. PhD thesis, London University. 314 pp.

Bateman, R.M., Hilton, J., 2009. Palaeobotanical systematics for the phylogenetic age: applying organ-species, form-species and phylogenetic species concepts in a framework of reconstructed fossil and extant whole plants. Taxon 58: 1254-1280.

798 Bateman, R.M., Rothwell, G.W., 1990. A reappraisal of the Dinantian floras at Oxroad Bay,
799 East Lothian, Scotland. 1. Floristics and the development of whole plant concepts.
800 Trans R Soc Edinb 81:127–159.
801 Bateman, R.M., Rothwell, G.W., Cleal, C.J., 1995. Oxroad Bay. Pp 127–139 in Cleal, C.J.,
802 Thomas, B.J. eds. Paleozoic paleobotany of Great Britain. Chapman & Hall, London.
803 Bateman, R.M., Scott, A.C., 1990. A reappraisal of the Dinantian floras at Oxroad Bay, East
804 Lothian, Scotland. 2. Volcanicity, palaeoenvironments and palaeoecology. Trans R
805 Soc Edinb 81:161–194.
806 Baxter, R.W., 1949. Some pteridosperm stems and fructifications with particular reference to
807 the Medullosaceae. Ann Miss Bot Gard 36:278-352.
808 Beck, C.B., 1960. The identity of *Archaeopteris* and *Callixylon*. Brittonia 12:351-368.
809 Beck, C.B., 1970. The appearance of gymnospermous structure. Bot Rev 45:379-400.
810 Beck, C.B., Schmid, R., Rothwell, G.W., 1982. Stelar morphology and the primary vascular
811 system of seed plants. Bot Rev 48:691-815, 913-931.
812 Becker, R.T., Kaiser, S.I., Aretz, M., 2016. Review of chrono-, litho- and biostratigraphy
813 across the global Hangenberg Crisis and Devonian–Carboniferous Boundary In:
814 Becker, R. T., Königshof, P. & Brett, C. E. (eds) 2016. Devonian Climate, Sea Level
815 and Evolutionary Events. Geol Soc Lond, Spec Publ 423:355–386.
816 Blanc-Louvel, C., 1966. Étude anatomique compare des tiges et des petioles d'une
817 ptéridospermée du Carbonifère de genre *Lyginopteris* Potonié. Mémoires du Muséum
818 National d'Histoire Naturelle 18:1-105.
819 Bridge, J.S., Van Veen, P., Matten., L.C., 1980. Aspects of the sedimentology, palynology

820 and palaeobotany of the Upper Devonian of southern Ireland Co. Kerry, Ireland. Geol
821 J 15:143-170.
822 Browne, M.A.E, Dean, M.T., Hall, I.H.S., Mcadam, A.M., Monro, S.K., Chisholm, J.I., 1999.
823 A lithostratigraphical framework for the Carboniferous rocks of the Midland Valley of
824 Scotland. Brit Geol Surv Res Rep RR/99/07.
825 Caplan, M.L. Bustin, R.M., 1999. Devonian-Carboniferous Hangenberg mass extinction
826 event, widespread organic-rich mudrock and anoxia: Causes and consequences.
827 Palaeogeogr Palaeoclimatol Palaeoecol 148:187–207.
828 Davies, A., Mcadam, A.D., Cameron, I.B., 1986. Geology of the Dunbar district. Memoir of
829 the British Geological Survey, Scotland, Sheet 33E and part of Sheet 41.
830 Diemer, J. A., Bridge, J.S., Sanderson D.J., 1987. Revised geology of Kerry Head, County
831 Kerry. Irish J Earth Sci. 8:113-138.
832 Dunn, M.T., 2006. A review of permineralized seed fern stems of the Upper Paleozoic. J
833 Torrey Bot Soc 133:20-32.
834 Dunn, M.T., Krings, M., Mapes, G., Rothwell, G.W., Mapes, R.H., Sun, K., 2003. *Medullosa*
835 *steinii* sp. nov., a seed fern vine from the Upper Mississippian. Rev Palaeobot Palynol
836 124:307-324.
837 Dunn, M.T., Rothwell, G.W., 2012. Phenotypic plasticity of the hydrasperman seed fern
838 *Tetrastichia bupatides* Gordon. Int J Plant Sci 173:823-834.
839 Eggert, D.A., 1961. The ontogeny of the Carboniferous arborescent Lycopsida. Palaeontogr
840 198B:43-92.

841 Galtier, J., 1974. Sur l'organisation de la fronde des *Calamopitys*, Ptéridospermales probables
842 de Carbonifère inférieur. CR Acad Sc Paris 279:975-978.
843 Galtier, J., 1977. *Tristichia longii*, nouvelle Ptéidospermale probable du Carbonifère de la
844 Montagne Noire. CR Acad Sci Paris 284:2215-2218.
845 Galtier, J., 1981. Structures foliaires de fougères et Ptéridospermales du Carbonifère inférieur
846 et leur signification évolutive. Palaeontogr 180B:1–38.
847 Galtier, J., 1982. New observations on the branching of Carboniferous ferns and
848 pteridosperms. Ann Bot 49: 737-746.
849 Galtier, J., 1988. Morphology and phylogenetic relationships of early pteridosperms. Pages
850 135–176 in Beck, C.B., ed. Origin and evolution of gymnosperms. Columbia
851 University Press, New York. 504 pp.
852 Galtier, J., 1999. Contrasting diversity of branching patterns in early ferns and early seed
853 plants. Pages 54–64 in Kurmann, M.H., Hemsley, A.R., ed. The evolution of plant
854 architecture. Roy Bot Gard Kew. 506 pp.
855 Galtier, J., 2013. Reinvestigation of the Carboniferous multiovulate cupule *Gnetoposis*
856 *elliptica* and its evolutionary significance. Int J Plant Sci.174:382–395
857 Galtier, J., Béthoux, O., 2002. Morphology and growth habit of *Dicksonites pluckenetii* from
858 the Upper Carboniferous of Graissessac (France). Geobios 35:535-535.
859 Galtier J, Meyer-Berthaud, B., 2006. The diversification of early arborescent seed ferns. J
860 Torrey Bot Soc 133:7–19.
861 Galtier, J., Scott, A.C., 1994. Anatomically preserved woody gymnosperms from the Viséan
862 of East Kirkton, West Lothian, Scotland. Trans R Soc Edinb, Ear Sci 84:261-266.

863 Gordon, W.T., 1938. On *Tetrastichia bupatides*, a Carboniferous pteridosperm from East
864 Lothian. Trans R Soc Edinb 59:351–370.
865 Gordon, W.T., 1941. On *Salapingostoma dasu*, a new Carboniferous seed from East Lothian.
866 Trans R Soc Edinb 60:227-264.
867 Hallé, F., Oldeman, R.A.A., Tomlinson, P.B., 1978. Tropical trees and forests. Springer-
868 Verlag, Berlin. 441 pp.
869 Hamer, J.J., Rothwell, G.W., 1988. The vegetative structure of *Medullosa endocentrica*
870 Baxter (Pteridospermopsida). Can J Bot 66: 375-387.
871 Higgs, K.T., Clayton, C., Keegan, J.B., 1988. Stratigraphic and systematic palynology of the
872 Tournaisian rocks of Ireland. Geol Surv Ireland Spec Pap 7:1-193.
873 Higgs, K.T., Prestianni, C. Streel, M Thorez, J., 2013. High resolution miospore stratigraphy
874 of the Upper Famennian of eastern Belgium, and correlation with the conodont
875 zonation. Geol Belg 16:84–94.
876 Hilton J., Bateman, R.M., 2006. Pteridosperms are the backbone of seed-plant phylogeny. J
877 Torrey Bot Soc 133:119–168.
878 Hirmer, M., 1933. Zur Kenntnis der Strukturbietenden Pflanzenreste des jüngeren
879 Palaeozoikums. 2: Über zwei neue, im mittleren Oberkarbon Westdeutschlands
880 gefundene Arten von *Heterangium shorense* Scott. Palaeontogr 78B:57-107.
881 Jennings, J.R., 1976. The morphology and relatioships of *Rhodea*, *Telangium*, *Telangiopsis*,
882 and *Heterangium*. Am J Bot 63:1119-1133.
883 Joy, K.W., Willis, A.J., Lacey, W.S., 1956. A rapid cellulose acetate peel method in
884 palaeobotany. Ann Bot NS 20:635–637.

885 Kaiser, S.I., Aretz, M., Becker, R.T., 2016. The global Hangenberg Crisis (Devonian-
886 Carboniferous transition): Review of a first-order mass extinction. Geol Soc Lon. Spec
887 Pub 423:387–437.
888 Kidston, R., 1923. Fossil Plants of the Carboniferous rocks of Great Britain. Memiors of the
889 Geol Surv Great Britain, Paleontol, Pt I, Pp. 1-110, Plates 1-110, and Part III, Pp. 199-
890 274, Plates 48-68.
891 Krings, M., Kerp, H., 1999. Morphology, growth habit, and ecology of *Blanzyopteris*
892 *praedentata* (Gothan) nov. comb., a climbing neuropterid seed fern from the
893 Stephanian of central France. Int J Plant Sci 160:603-619.
894 Long, A.G., 1961. "*Tristichia ovense*" gen. et sp. nov., a protostelic Lower Carboniferous
895 pteridosperm from Berwickshire and East Lothian, with an account of some associated
896 seeds and cupules. Trans R Soc Edinb 64:477-492.
897 Long, A.G., 1963. Some specimens of *Lyginorachis papilio* Kidston associated with stems of
898 *Pitys*. Trans R Soc Edinb 65:211-224.
899 Long, A.G., 1975. Further observations on some Lower Carboniferous seeds and cupules.
900 Trans R Soc Edinb 69: 267-293.
901 Long, A.G., 1976. *Calathopteris heterophylla* gen. et sp. nov., a Lower Carboniferous
902 pteridosperm bearing two kinds of petioles. Trans R Soc Edinb 69:327-336.
903 Mapes, G., Rothwell, G.W., Howarth, M.T., 1989. Evolution of seed dormancy. Nature
904 337:645-646.

905 Marshall, J.A.E., Lakin, J., Troth, I., Wallace-Johnson, S.M., 2020. UV-B radiation was the
906 Devonian-Carboniferous boundary terrestrial extinction kill mechanism. Sci. Adv.
907 2020; 6: eaba0768.
908 Masselter, T., Rowe, N.P., Speck, T., 2007. Biomechanical reconstruction of the
909 Carboniferous seed fern *Lyuginopteris oldhamia*: Implications for growth from
910 reconstruction and habit. Int J Plant Sci 168:1177–1189.
911 Matten, L.C., Lacey, W.S., Edwards, D., 1975. Discovery of one of the oldest gymnosperm
912 floras containing cupulate seeds. Phytologia 32:299-303.
913 Matten, L.C., Lacey, W.S., Lucas, R.C., 1980a. Studies on the cupulate seed genus
914 *Hydrasperma* Long from Berwickshire and East Lothian Scotland and County Kerry
915 in Ireland. Bot J Linn Soc 81:249-273.
916 Matten, L.C., Lacey, W.S., May, B.I., Lucas, R.C., 1980b. A megafossil flora from the
917 Uppermost Devonian near Ballyheigue, Co. Kerry, Ireland. Rev Paleobot Palynol
918 29:341-351.
919 Matten, L.C., Tanner, W.R., Lacey, W.S., 1984. Additions to the silicified Upper
920 Devonian/Lower Carboniferous flora from Ballyheigue, Ireland. Rev Palaeobot
921 Palynol 43:303–320.
922 May, B.I., Matten, L.C., 1983. A probable pteridosperm from the uppermost Devonian near
923 Ballyheigue, County Kerry, Ireland. Bot J Linn Soc 86:103–123.
924 Meade, L.I., Plackett, A.R.G., Hilton, J., 2021. Reconstructing development of the earliest
925 seed integuments raises a new hypothesis for the evolution of ancestral seed-bearing
926 structures. New Phytol 229:1782-1794.

927 Meyer-Berthaud, B., 1989. First gymnosperm fructifications with trilete prepollen.
928 Palaeontogr 211B:87-112.
929 Millay, M.A., Taylor, T.N., 1979. Paleozoic seed fern pollen organs. Bot Rev 45:301-375.
930 Monaghan, A.A., M. A. E. Browne, M.A.E., Barfod, D.N. 2014. An improved chronology for
931 the Arthur's Seat volcano and Carboniferous magmatism of the Midland Valley of
932 Scotland. Scot J Geol 50:165–172,
933 Monaghan, A.A., Parrish, R.R., 2006. Geochronology of Carboniferous–Permian volcanism
934 in the Midland Valley of Scotland: Implications for regional tectono-magmatic
935 evolution and the numerical timescale. J Geol Soc Lond 163:15–28.
936 Niklas, K.J., 1983. The influence of Paleozoic ovule and cupule morphologies on wind
937 pollination. Evol 37:968-986.
938 Niklas, K.J., 1985. The aerodynamics of wind pollination. Bot Rev 51:328-386.
939 Oliver, F.W., Scott, D.H., 1904. On the structure of the Paleozoic seed *Lagenostoma lomaxi*,
940 with a statement of the evidence upon which it is referred to *Lyginodendron*. Phil
941 Trans R Soc Lond B 197:193–247.
942 Pfefferkorn, H.W., Gillespie, W.H., Resnick, D.A., Scheihing, M.H. 1984. Reconstruction and
943 architecture of medullosan pteridosperms (Pennsylvanian). Mosasaur 2:1-8.
944 Prestianni, C., Sautois, M., Denayer, J., 2016. Disrupted continental environments around the
945 Devonian Carboniferous Boundary: Introduction of the tener event. Geol. Belg. 19,
946 135–145.
947 Retallack, G.J., Dilcher, D.L., 1988. Reconstructions of selected seed ferns. Ann Missouri Bot
948 Gard 75:1010-1057.

949 Rothwell, G.W., 1971. Additional observations on *Conostoma anglo-germanicum* and *C.*
950 *oblongum* from the Lower Pennsylvanian of North America. Palaeontogr 131B:167-
951 178.
952 Rothwell, G.W., 1975. The Callistophytaceae (Pteridospermopsida). I. Vegetative structures.
953 Palaeontogr 151B:171–196.
954 Rothwell, G.W., 1976. Primary vasculature and gymnosperm systematics. Rev Palaeobot
955 Palynol 22:193-206.
956 Rothwell, G.W., 1986. Classifying the earliest gymnosperms. pp. 137-161 in Spicer, R.A.,
957 Thomas, B.A. eds., Systematic and taxonomic approaches in Paleobotany. Sys Assoc
958 Spec Vol 31, Linn Soc Lond, Academic Press. 350 pp.
959 Rothwell, G.W., 2021. The evolution of stelar architecture. In: Tomescu, A.M.F., 2021. The
960 stele – a developmental perspective on the diversity and evolution of primary vascular
961 architecture. Biol Rev. doi: 10.1111/brv.12699.
962 Rothwell, G.W., Scheckler, S.E., 1988. Biology of ancestral gymnosperms. Pages 85-134 in
963 Beck, C.B., ed. Origin and evolution of gymnosperms. Columbia University Press,
964 New York. 506 pp.
965 Rothwell, G.W., Scheckler, S.E., Gillespie, W.H., 1989. *Elkinsia* gen. nov., a Late Devonian
966 gymnosperm with cupulate ovules. Bot Gaz 150:170-189.
967 Rothwell, G.W., Scott, A.C., 1985. Ecology of Lower Carboniferous plant remains from
968 Oxroad Bay, East Lothian, Scotland. Am J Bot 72:899.

969 Rothwell, G.W., Scott, A.C., 1992. *Stamnostoma oliveri*, a gymnosperm with systems of
970 ovulate cupules from the Lower Carboniferous (Dinantian) floras at Oxroad Bay, East
971 Lothian, Scotland. Rev Palaeobot Palynol 72: 273-284.
972 Rothwell, G.W., Serbet, R., 1994. Lignophyte phylogeny and the evolution of
973 spermatophytes: A numerical cladistics analysis. Sys Bot 19:443-482.
974 Rothwell, G.W., Taylor, T.N., 1972. Carboniferous pteridosperm studies: morphology and
975 anatomy of *Schopfiastrum decussatum*. Can J Bot 50:2649-2658.
976 Rothwell, G.W., Wight, D., 1989. *Pullaritheca longii* gen. nov. and *Kerrya mattenii* gen. et
977 sp. nov., Lower Carboniferous cupules with ovules of the *Hydrasperma*-type. Rev
978 Palaeobot Palynol 60:295-310.
979 Rothwell, G.W., Wyatt, S.W., Tomescu, A.M.F., 2014. Plant evolution at the interface of
980 paleontology and developmental biology: an organism centered paradigm. Am J Bot
981 101:899-913.
982 Rowe, N.P., 1988. New observations on the Lower Carboniferous pteridosperm
983 *Diplopteridium* Walton and an associated synangiate organ. Bot J Linn Soc 97:125-
984 158.
985 Sanders, H., Rothwell, G.W., Wyatt, S.E., 2009. Key morphological alterations in the
986 evolution of leaves. Int J Plant Sci 170:860-868.
987 Schopf, J.M., 1975. Modes of fossil preservation. Rev Palaeobot Palynol 20: 27-53.
988 Scott, A.C., 1985. Distribution of Lower Carboniferous Floras in northern Britian. Compte
989 Rendue, IX International Congress on Carboniferous Stratigraphy and Geology.
990 Illinois 1979, 5:77-82.

991 Scott, A.C., 1990. Preservation, evolution, and extinction of plants in Lower Carboniferous
992 volcanic sequences in Scotland. In Lockley, M.G., Rice, A. eds. Volcanism and fossil
993 biotas. Geol Soc Am Spec Pap 244:25–38.
994 Scott, A.C., Galtier, J., Clayton, G., 1984. Distribution of anatomically preserved floras in the
995 Lower Carboniferous in western Europe. Trans R Soc Edinb 73:311–340.
996 Scott, A.C., Hilton, J., Galtier, J., Stampanoni, M., 2019. A charcoalified ovule adapted for
997 wind dispersal and deterring herbivory from the Late Viséan (Carboniferous) of
998 Scotland. Int J Plant Sci 180:1059-1074.
999 Scott, A.C., Rex, G.M., 1987. The accumulation and preservation of Dinantian plants from
1000 Scotland and its borders. In: Adams, A.E., Miller, J., Wright, V.P. (eds). European
1001 Dinantian Environments. Geol J Spec Issue 12:329-344.
1002 Serbet, R., Rothwell, G.W., 1992. Characterizing the most primitive seed ferns. I. A
1003 reconstruction of *Elkinsia polymorpha*. Int J Plant Sci 53:602-621.
1004 Serbet, R., Rothwell, G.W., 1995. Functional morphology and homologies of gymnospermous
1005 ovules: Evidence from a new species of *Stephanospermum* (Medullosales). Can J Bot
1006 73:650-661.
1007 Seward, A.C., 1911. Fossil Plants. Vol. III. Cambridge Univ Press. 656 pp.
1008 Silvestro, D., Cascales-Miñana, B., Bacon, C.D., Antonelli, A., 2015. Revisiting the origin
1009 and diversification of vascular plants through a comprehensive Bayesian analysis of
1010 the fossil record. New Phytol 207:425–436.
1011 Speck, T, Rowe, N.P., 1994. Biomechanical analysis of *Pitus dayi*: early seed plant vegetative
1012 morphology and its implications on growth habit. J Plant Res 107:443–460.

1013 Stein, W.E., Jr., Wight, D.C., Beck, C.B., 1982. Techniques for preparation of pyrite and
1014 limonite permineralizations. Rev Palaeobot Palynol 36:185-194.
1015 Stephenson, M.H., Williams, M., Monaghan, A.A., Arkley, S., Smith, R.A., Dean, M.,
1016 Browne, M.A.E., Leng, M., 2004. Palynomorph and ostracod biostratigraphy of the
1017 Ballagan Formation, Midland Valley of Scotland, and elucidation of intra-Dinantian
1018 unconformities. Proc Yorkshire Geol Soc 55:131–143.
1019 Stevenson, D.W., 2020. Observations on vegetative branching in cycads. Int J Plant Sci
1020 181:564–580.
1021 Streel, M., 2009. Upper Devonian miospore and conodont zone correlation in western Europe.
1022 Geol Soc Lond Spec Pub 314:163-176.
1023 Stewart, W.N., Rothwell. G.W., 1993. Paleobotany and the evolution of plants. Cambridge
1024 University Press, Cambridge. 521 pp.
1025 Stidd, B.M., Phillips, T.L., 1973. The vegetative anatomy of *Schopfiastrum decussatum* from
1026 the Middle Pennsylvanian of the Illinois Basin. Am J Bot 60:463–474.
1027 Taylor, T.N., Taylor, E.L., Krings, M., 2009. Paleobotany. The biology and evolution of fossil
1028 plants. 2nd ed. Elsevier, New York. 1230 pp.
1029 Tomescu, A.M.F., Rothwell, G.W., Mapes, G., 2001. *Lyginopteris royalii* sp. nov. from the
1030 Upper Mississippian of North America. Rev Palaeobot Palynol 116:159-173.
1031 Zodrow, E.L., Tenchov, Y.G., Cleal, C.J., 2007. The arborescent *Linopteris oblique* plant
1032 (Medullosales, Pennsylvanian). Bull Geosci 82:51-84.
1033

Figure caption

Figure 1. Suggested reconstruction of *Tetrastichia bupatides* as a small, upright plant with frond-borne reproductive organs. See text for details.

Plate captions

Plate I.

Plant-bearing volcanic deposits of Oxroad Bay, East Lothian, Scotland. 1. Main plant-bearing sequences in the base of the Garleton Hills Volcanic Formation. Plant-bearing lens collected by Gordon and ourselves (A), together with another plant-bearing lens (B) as collected in 1984; 2. Plant-bearing lens collected by Gordon, with hammer for scale. Reprinted from Plate I, Figure 1 of Gordon, 1938; 3. Plant-bearing lens of Gordon (1938) as collected in 1984. 4. Thin section of plant-bearing tuffs showing graded beds of volcaniclastic ashes and permineralized plants. ACS slide OXC2021-1; 5. Thin section of plant bed from cliff section near A in Figure 1. ACS slide OXC2021-2; 6. Thin section of *Tetrastichia bupatides* from Exposure A in Figure 1. ACS slide OXC2021-3.

Plate II.

Distal frond pinnae and pinnules of *Tetrastichia bupatides*, and pinna anatomy of *Triradioxylon primaevum* frond segments. All sections from block 712 I. 1. Pinnae of *Tetrastichia bupatides* (toward top and center) and *Triradioxylon primaevum* (Tri). Note that *T. bupatides* pinnae have narrower and more dissected zone of hypodermal sclerenchyma, and thinner-walled ground parenchyma than *Triradioxylon primaevum* pinna. Note also that some

cells of parenchymatous ground tissue in *T. bupatides* pinnae have black contents, whereas those of *T. primaevum* do not. A top #314 x 7; KUNH slide 30,860. Scale bar = 2 mm; 2. Cross section of *T. bupatides* pinnule showing oval lobes (green arrowheads) aligned in row. Arrow identifies branching lobe below level of dichotomy. Note also, relatively distal pinna of *Triradioxylon primaevum* (Tri). A bot #252 x 8; KUNH slide 30,866. Scale bar = 2 mm; 3. Forking lobe of *T. bupatides* pinnule. Note black contents in ground parenchyma and hypodermal sclerenchyma restricted to area of lobe separation at level of branching (arrow). A bot #23 x 15; KUNH slide 30,863. Scale bar = 0.5 mm; 4, Pinnule in cross section showing forking lobes in row (green arrowheads). A bot 23 x 10; KUPB slide 30,863. Scale bar = 2 mm; 5. Pinnae (cross sections) and pinnule lobes (oblique sections) of *T. bupatides*), as compared to pinna of *Triradioxylon primaevum* (Tri). . 6. Longitudinal section of incomplete pinnule showing five forks (at arrows) in elongated narrow lobes. A bot #6 x 8. Scale bar = 2 mm. slide 30,861; 7A bot #24x 8.5. Scale bar = 2 mm. KUNH slide 30,864; 7. Pinna (tertiary, with adaxial surface upward) enlarged from Plate II, 5. Five lobed trace (blue arrowheads) producing terete pinnule bundle (red arrowhead). Both pinna rachis and pinnule base with hypodermal sclerenchyma. Note black contents in ground parenchyma cells, and almost complete absence (except at arrow) of hypodermal sclerenchyma distal to basal fork of pinnule (top of photo). 8. Slightly oblique cross section of pinnule lobe with terete trace (red arrowhead), dark contents in some mesophyll cells, and incompletely preserved epidermis. A bot #252x 30. Scale bar = 0.5 mm. KUNH slide 30,866; 9. Cross section of somewhat degraded pinnule lobe with no hypodermal sclerenchyma, irregular outer margin, terete

bundle (red arrowhead), and large percentage of ground parenchyma cells with black contents. A bot #24x 40. Scale bar = 0.5 mm; 10. KUNH slide 30,864.

Plate III.

Rooting structures of *T. bupatides*. 1-5, basipetal series of cross sections of branching taproot; 1. Near apical section distal to mature tissues. 712 I C top #222 x 12. Scale bar = 1 mm. KUNH slide 30,799; 2. Section 4 mm from apex showing abundant wood. 712 I C top #178 x 12. Scale bar = 1 mm. KUNH slide 30,800; 3. Section 7 mm from apex, at level of divergence of two branch roots. 712 I C top #103 x 8. Scale bar = 1 mm. KUNH slide 30,801; 4. Cross section showing tetrarch actinostele, abundant wood, and outer cortex of taproot. 712 I A top #290 x 9. Scale bar = 1 mm. KUNH slide 30,802; 5. *Amyelon*-type taproot in organic connection to stem base identifiable as *Tetrastichia* by characteristic *Dictyoxylon*-type outer cortex (green arrowheads). 712 II A top #59 x 12. Scale bar = 1 mm. KUNH slide 30,803; 6. Cross section of stem (at left) at level of frond divergence (at right), the juncture of which is intersected by *Amyelon*-type root that appears to have diverged from base of rachis. 712 II A bot #86 x 8. Scale bar = 1 mm. KUNH slide 30, 804; 7. Cross section of near basal level of stem showing diverging rachis (upper left), and with well-preserved primary cortex, continuous cylinder of thick secondary vascular tissue, diverging adventitious root (r), and root traces (red arrowheads) at outer margin of wood. Rachis trace and four-lobed trace to more distal frond in inner cortex (boxes). Note disruption of radial rows of tracheids, revealing position of diverging frond trace (at blue arrow). Note also, incompletely preserved primary tissues at center of stem do not show structure of stele. SIPC 666.14 D-1-C # 1 x 9.5.

Scale bar = 2 mm. KUNH slide 30,806; 8. Enlargement of adventitious root in cortex of stem in Plate III, 7, showing tetrarch protostele (with one short rib) and primary cortex. SIPC 666.14 D-1- # 1 x 19. Scale bar = 1 mm. KUNH slide 30,806.

Plate IV.

Pollen organ structure and attachment. All sections from block 712 I; 1. Composite figure of aggregate pollen organ attached distally to tertiary pinna. Arrows indicate positions from which enlargements (in Plate III, 2-6) were made. A top #s 3-9, 14, 42, 83, and 233 x 3. Scale bar = 1 cm. KUNH slides 30,820-30,830, 30,838, 30,845, 30,858.; 2. Oblique section of four-lobed pinna trace in oblique cross section. A top #7 x 28. Scale bar = 0.5 mm. KUNH slide 30,824; 3. Same pinna trace as in Plate III, 2, but divided into three segments. A top #3 x 20. Scale bar = 0.5 mm. KUNH slide 30,805; 4. More proximal level of pinna in longitudinal section showing central trace, ground parenchyma cells with black contents, and narrow zone of hypodermal sclerenchyma. A top #83 x 10. Scale bar = 1 mm. KUNH slide 30,845; 5. Pinnule with single terete trace (pt) diverging from pinna. A top #3 x 8. Scale bar = 2 mm. KUNH slide 30,820; 6. Adjacent section of same elongated pinnule as in Plate III, 5, showing central trace (pt) and ground parenchyma cells with black contents. A top #4 x 7. Scale bar = 2 mm. KUNH slide 30,821; 7. Enlargement of aggregate pollen organ in Plate IV, 1 showing antepenultimate pinna (app), penultimate pinna (pp), basal cushions of several simple synangia, and other simple synangia in various planes of section. Note dense trichomes surrounding sporangia. A top #233 x 9. Scale bar = 2 mm. KUNH slide 30,858; 8. Penultimate pinna (pp) of aggregate pollen organ showing zig-zag configuration caused by unequal

forking to produce ultimate segment with terminal simple synangia. A top #284 x 6. Scale bar =2 mm. KUNH slide 30,859; 9. Ultimate segment of aggregate pollen organ, with single vascular bundle (arrow), forking from penultimate pinna. Note sporangia diverging from basal cushion in longitudinal section, and adjacent simple synangium with six sporangia (blue numbers) in cross section. A bot #184 x 14. Scale bar = 2 mm. KUNH slide 30,856; 10. Section through ultimate segments of aggregate synangium, with inverted basal cushions surrounding sporangia of adjacent simple synangia. A bot #184 x 9. Scale bar = 2 mm. KUNH slide 30,856; 11. Cross section through central region of simple synangium with six sporangia (blue numbers). Note sporangia are not attached to each other at this level. A bot #123 x 22. Scale bar = 0.5 mm. KUNH slide 30,807; 12. Sporangium (green arrow) surrounded by dense trichomes in cross section. Segment of trichome in longitudinal section at red arrowhead. A bot #174 x 40. Scale bar = 0.2 mm. KUNH slide 30,855; 13. Several simple synangia showing sporangia (s) attached to cushion (c). Note sporangia are not attached to each other laterally. A bot #96 x 9. Scale bar = 2 mm. KUNH slide 30,808; 14. Longitudinal view of two sporangia attached to cushion (C), showing rounded apices, isodiametric cells of epidermis (arrow), and elongated black coalified cells of sporangial walls. 712 I A top #184 x 30. Scale bar = 0.5 mm. KUNH slide 30,856.

Plate V.

Cupule attachment, enclosed ovules, and stalked *Eosperma oxroadense*. All sections from block 712 I; 1-5. Acropetal series of stem cross sections showing *Calathospermum fimbriatum* cupule and frond rachis diverging from *Tetrastichia bupatides* stem. Fig.1 is most proximal

level of internode; Fig. 5 is most distal. Fig. 5 is just distal to rachis trace divergence (where rachis is out of section). Both appendages are bent backward. Cupule stalk broken at level of divergence from stem, remaining attached only by narrow strip of tissue (Figs. 8 at arrow, and 9); 1. Cross section of stem below node of cupule attachment, and dividing cupule bent-backward. 712 I B top #218 x 2.8. Scale bar = 1 cm. UKNH slide 30,813; 2. Cross section of stem closer to node than Plate V, 1, showing undivided cupule base. 712 I B bot #37 x 2.8. Scale bar = 1 cm. KUNH slide 30,814; 3. Section distal to Fig. 2 (just below node), showing stem, cupule stalk, and rachis. Note tissue extending away from cupule base. 712 I C top #18 x 3.2. Scale bar = 1 cm. KUNH slide 30,809; 4. Near nodal level of stem with bent-back rachis partly attached to stem and cupule stalk adjacent to stem. 712 I C top #111 x 3.5. Scale bar = 1 cm. KUNH slide 30,810; 5. Cross section of stem in nodal region, immediately distal to divergence of rachis, and near level of cupule attachment. Note cortical tissue of stem (arrow) extending toward cupule stalk at upper left. Blue lines indicate radii upon which rachis (vertical line) and cupule stalk (bisected diagonal line) diverge. Double-headed arrow emphasizes that these angles of divergence are offset by ~35-40^{o}. 712 I C bot #260 x 2.9. Scale bar = 1 cm. KUNH slide 30,819; 6. Cupule stalk near base, showing U-shaped arrangement of bundles and ground parenchyma. Note some parenchyma cells of ground tissue have black contents. 712 I C top #216 x 12. Scale bar = 1 mm. KUNH slide 30,816; 7. Stem and cupule stalk at distal level of nodal region. Note stem tissue extending toward cupule stalk. Blue line indicates radius upon which cupule divergence occurs. 712 I C top #234 x 3.6. Scale bar = 5 mm. KUNH slide 30,818; 8. Stem and cupule stalk at level of narrow tissue continuity (arrow). 712 I C top #228 x 8. Scale bar = 2 mm. KUNH slide

30,817; 9. Enlargement of tissue continuity in Fig. 8, showing cellular composition of attachment. 712 I C top #228 x 16. Scale bar =1 mm. KUNH slide 30,817; 10. Cross section at midlevel of cupule showing several enclosed ovules, most of which are assignable to *Eosperma oxroadense*. 712 I B top #13 x 2. Scale bar = 5 mm. Slide 30,812; 11. Enlargement of ovules within *Calathospermum* cupule showing at least four specimens of *E. oxroadense* and other ovules in various planes of section. 712 I B top #13 x 4.5. Scale bar = 2 mm. KUNH slide 30,812; 12. *Eosperma oxroadense* in mid-longitudinal section of minor plane, attached to terete stalk. 712 I 582 B bot #1 x 8. Scale bar = 2 mm. KUNH slide 30,806; 13. Enlargement of terete stalk in Plate V, 12, showing cells of parenchymatous mesophyll, some of which have black contents. 712 I 582 B bot #5 x 16. Scale bar = 1 mm. KUNH slide 30,810; 14. Cross section of smallest type axis attached to central region of *Calathospermum fimbriatum* cupule at same magnification as stalk in Plate V, 10. Note similarity of size and histology as compared to stalk to which *E. oxroadense* is attached (Fig. 13). 712 I B top #13 x 16. Scale bar =1 mm. KUNH slide 30,812.

Figure 1

Click here to access/download;Figure;Tetrastichia bupatides reconstruction.tif

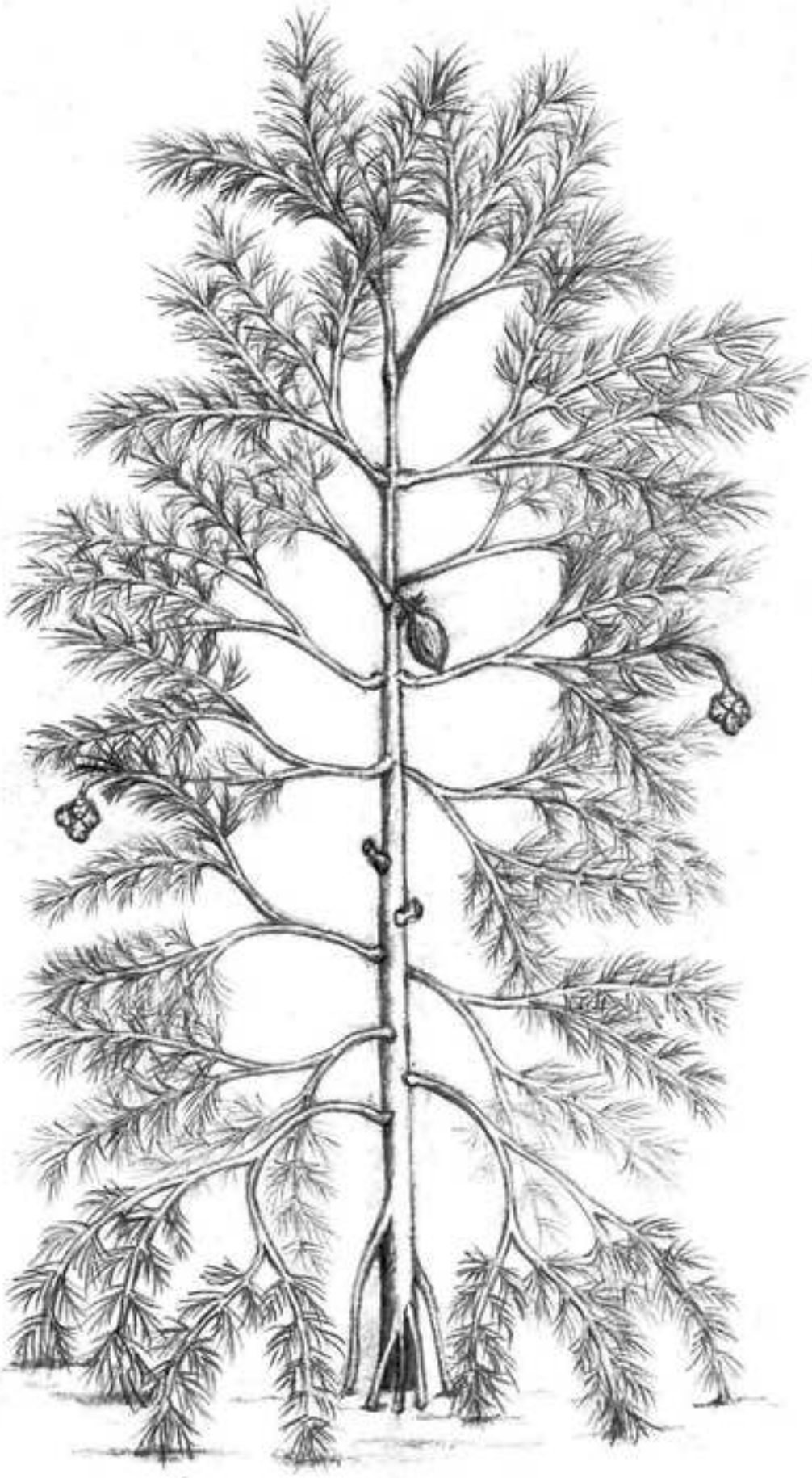

Plate I

Click here to access/download;Figure;Plate I.tif

Plate II

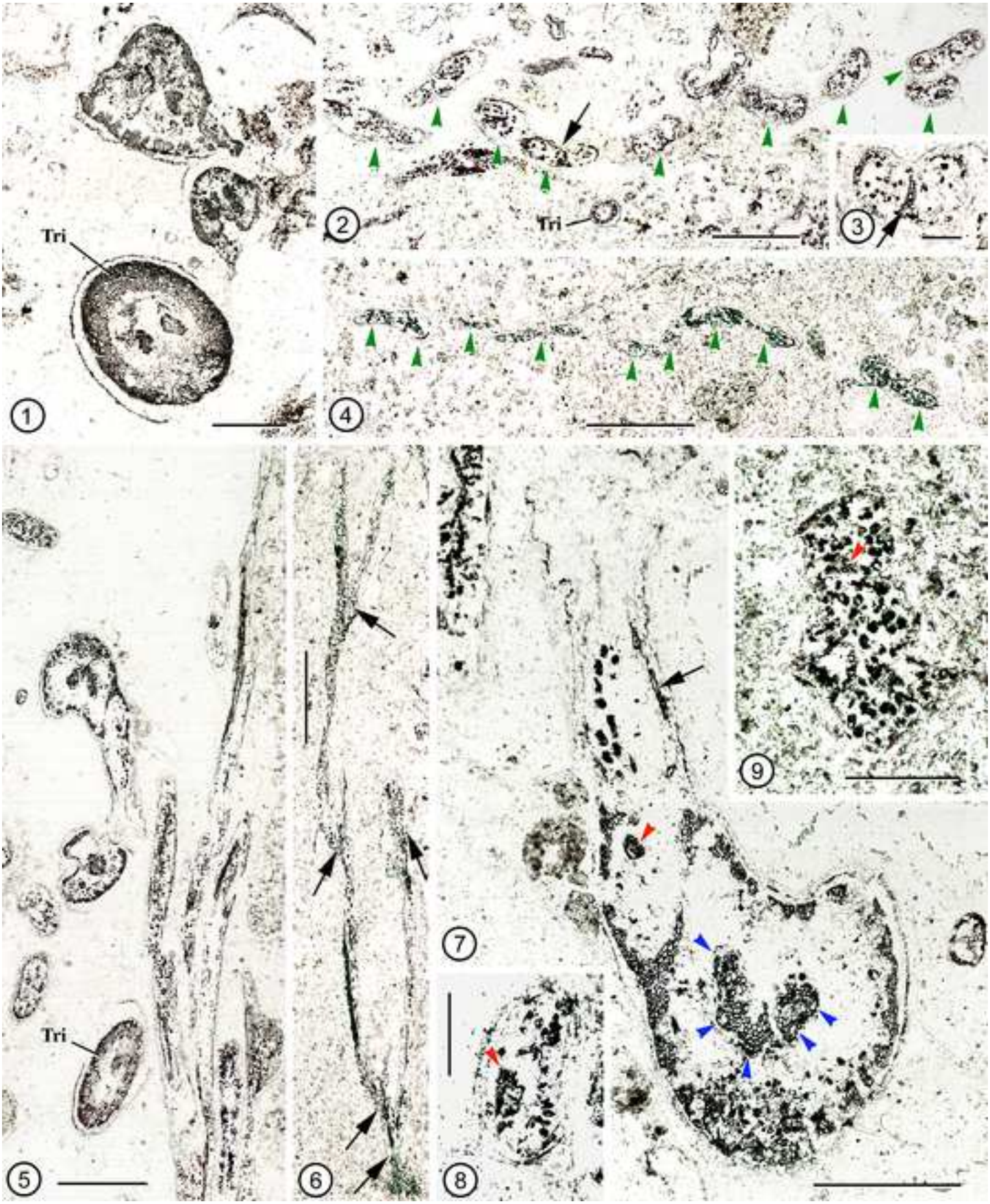

Plate III

Click here to access/download;Figure;Plate III.tif

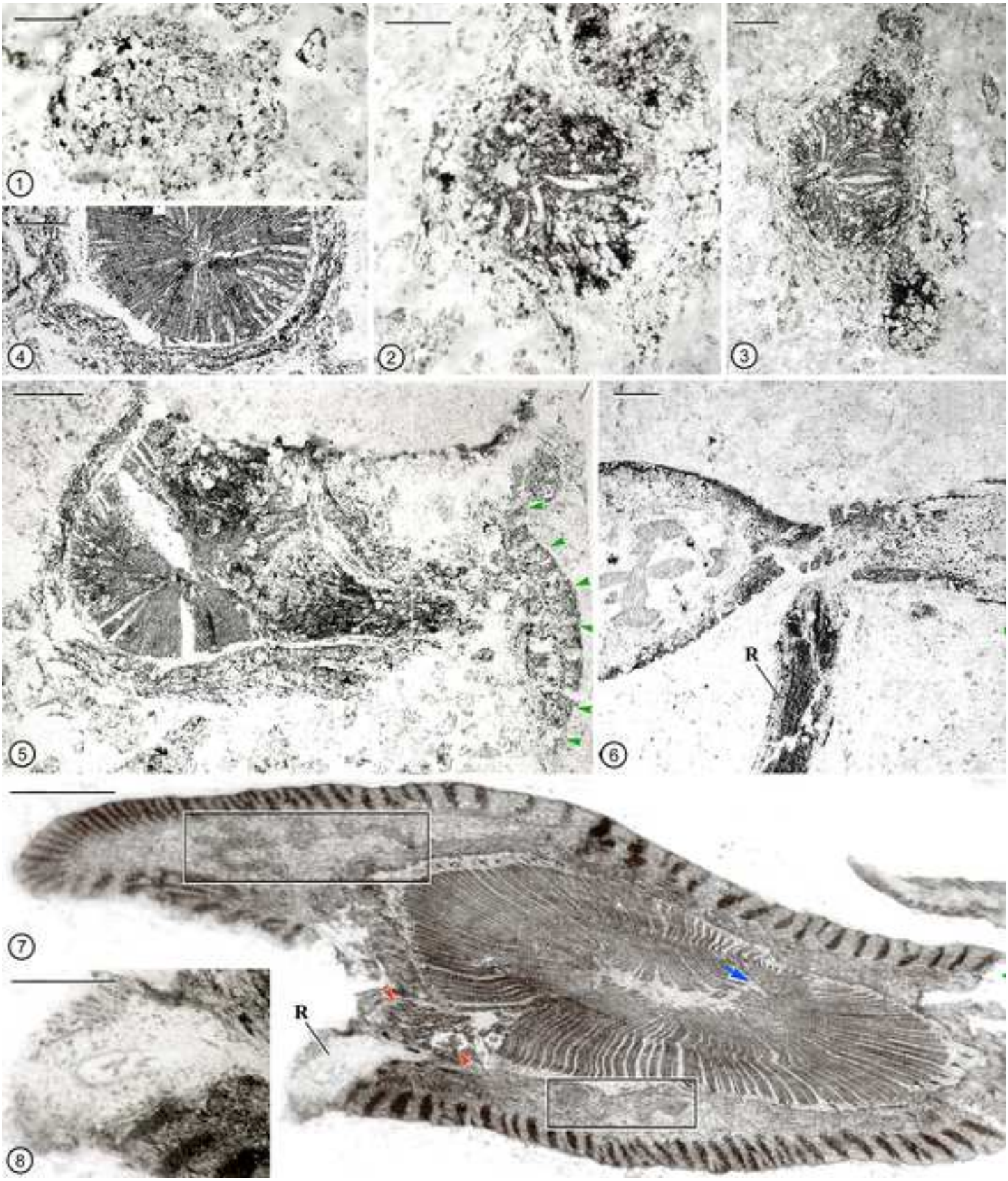

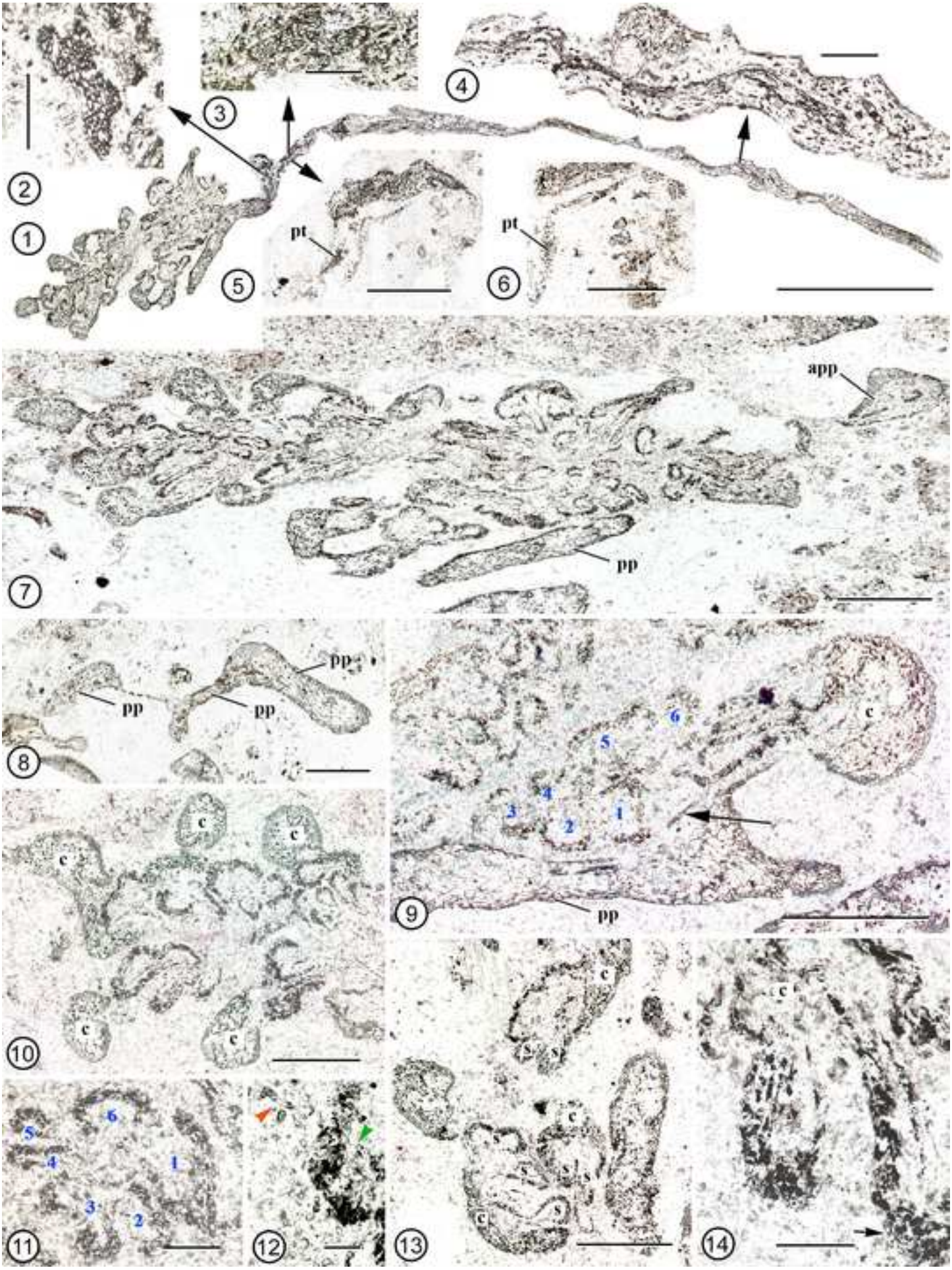

Plate V

Click here to access/download;Figure;Plate V.tif

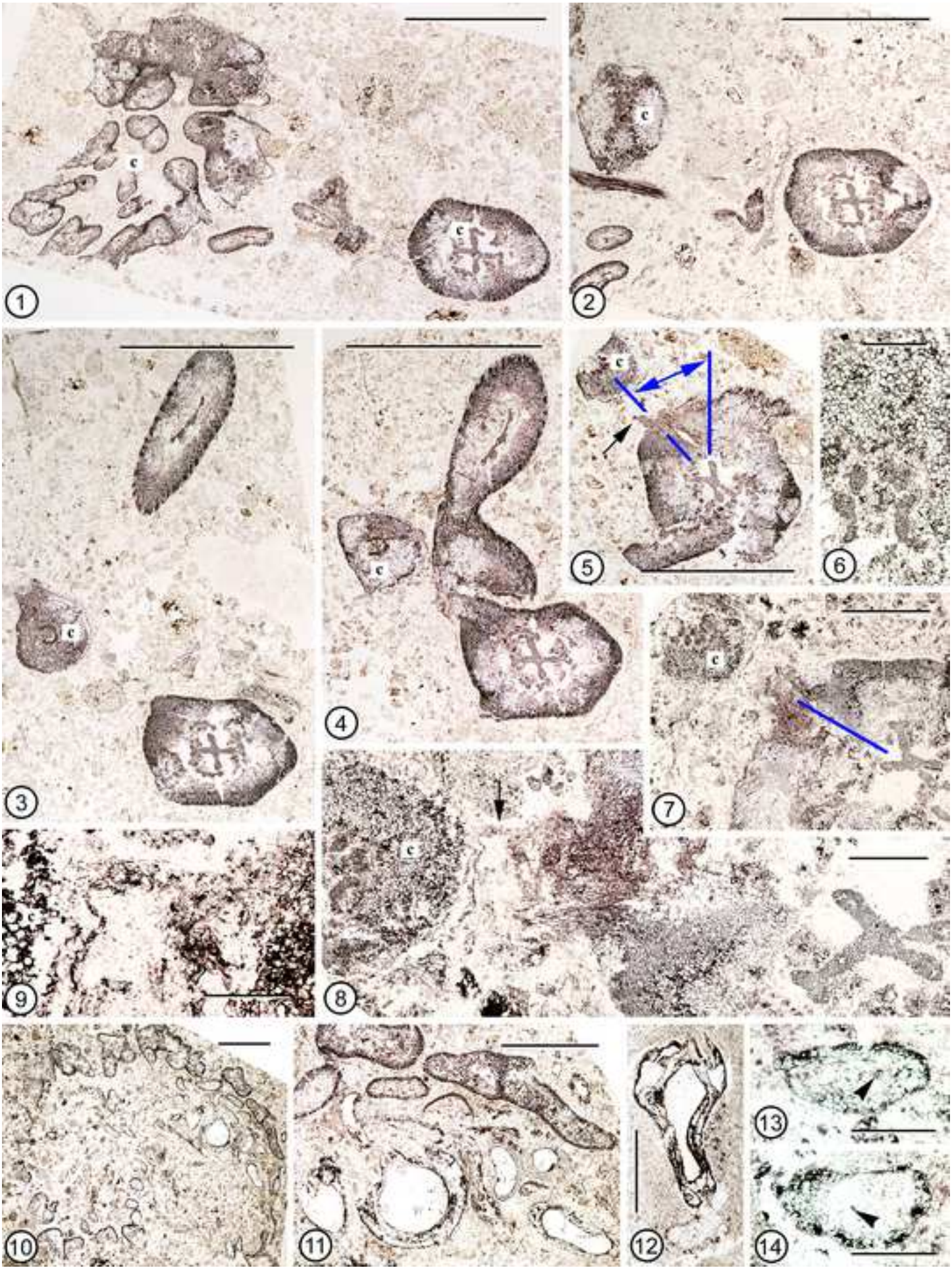

Table 1. Specimens used to develop a whole plant concept for *Tetrastichia bupatides*

Publication	Organ Taxa Included	Material Source	Repository and Material	Specimen/block Numbers
Gordon, 1933	*Tetrastichia bupatides*	[1]A	[2]LNHM (Gordon Collection) One large block, broken into several segments. Segments recut as several numbered blocks. Gordon prepared petrological thin sections; subsequent workers made peels.	Gordon block plus peels and slide Nos. 1,832-2,428
Barnard, 1959	*Eosperma oxroadense*	[1]A	[2]LNHM (Gordon Collection) Blocks, peels, and sides, including new preparations	Gordon block plus peels and slide Nos. 1,994, 1,995, 2,036, 2,037, 2,141-2,148, Peels 2,113-2,189.
Barnard, 1960a	*Calathospermum fimbriatum*	[1]A	[2]LNHM (Gordon Collection) Blocks, peels, and sides, including new preparations	Gordon block plus peels and slides Nos. 2,190-2,385
Barnard, 1960b	*Amyelon* sp. *C. fim briatum, E. oxroadense, Lyginorachis* spp., *T. bupatides*	[1]A	[2]LNHM (Gordon Collection) Blocks, peels, and sides, including new preparations	Gordon block plus peels and slides from Gordon Collection. Figured slides are Nos. 2,279-2,385
Barnard, 1962	*Amyelon. bovius*	[1]A	[2]LNHM (Gordon Collection) Blocks, peels, and sides, including new preparations	Gordon block plus peels and slide Nos. 2,390-2,428.
Long, 1975	*Calathospermum fimbriatum*	[1]A	[2]GNMH (Albert Long Slide Collection)	Slide Nos. 5,619-5,674, 6,297-6,341, 8,975-9,185.
Long, 1979	*C. fimbriatum*	[1]A	[2]GNMH (Albert Long Slide Collection)	Slide Nos. 10,114-10,162, 10,252-10,260, 11,225-11,245,

				11,668-11,671, 11,674-11,688, 11,699-11,710.
Matten et al., 1980	*T. bupatides*	[1]B	[2]KUNH, Paleobotanical Collections	Matten Collection Nos. 13,957 = 666.013, KUPB 13,959 = 666.015, KUPB 13,960 = 666.016, KUPB 13,963 = 666.019, KUPB 14,007 = 666.066, KUPB 14,031 = 666.201, KUPB 14,052 = 681.001, KUPB 14,070 = 666.005 KUPB 14,081 = 682.030, KUPB 14,089 = 682.038, KUPB 14,100 = 682.051
May et al., 1983	*T. bupatides*	[1]B	[2]KUNH, Paleobotanical Collections	Ibid.
Matten et al., 1984	*T. bupatides*		[2]UKNH, Paleobotanical Collections	Ibid.
Bateman and Rothwell, 1990	*Amyelon* sp. *C. finbriatum,* *E. oxroadense,* Pollen organ *T. bupatides*	[1]A	RHC LNHM RHC RHC LMNH	OBD (2.30) 198eb/1 Gordon Slide 2,235 ACS 672 cB, OBC 027eB ACS 666B, OBD (2.26) 188c1T/C, OBD (2.26)188c1T/12+17 Gordon Slides from 1,832-2,428
Dunn and Rothwell, 2012	*T. bupatides*	[1]A	[2]KUNH, Paleobotanical Collections	712-1-3-Bt36, 223-6-B-1-17, 712-2-11-Ab150, 610-1-Dt3, 712-1-4- Ct149, 610-2-Dt8, 610-2-Cb38, 610-2-Ct162, 712-2-7-Ct3, 712-2-7-Bt99, 712-2-7-At86, 610-2-Dt202, 662-1-b, 605-1-

				E-1-12, 712-1-5-At68, 712-1-5-At182, 712-1-18-Bb22, 223-6-Ab2, 605-I-D-2-55, 605-2-D-1-7, 800-14-1, 605-I-B-1-19, 715-25-G-1-17, 662-A-2, 610-2-Dt124, 605-1-F-5-12, 605-1-F-5-2, 605-2-A-1-5, 712-1-5-Ab24, 712-1-3-At19, 605-2-B-5-15, 712-1-3-Ab60, 712-1-3-Ab231, 712-1-3-Ab252, 712-1-3-Ab310, 610-3-Ct189, 610-3-Ct179, 712-1-19-At290, 712-1-19-At65, 610-21-Dt84, 610-21-Dt98, 610-22-Cb110, 610-21-Bb191.
Rothwell, et al., current study	*Amyelon* sp. *C. finbriatum,* *E. oxroadense,* *Lyginorachis* spp., *Salpingostoma dasu* *T. bupatides*	[1]A, B	[2]LNHM, UKNH; ACS	All blocks, peels, and slides listed above, plus ACS slides OXC2021-1 - OXC2021-3, and UKNH block and collection numbers numbers: block 223 = 17,286, 288 = 17,291, 605 = 17,338, block 610 = 17,343, block 672 = 17,395, block 712 I = 17,434, bock 712 II = 17,434, block 715 = 17,437 , block 719 = 17,441, block 733 = 17,455, block 772 = 17,494: and UKNH slides 30,799 - 32,134 and 35,949 - 36,010.

[1]A = Oxroad Bay, Assemblage A; B = Ballyheige, Kerry County, Ireland. See text for details.

[2]LMNH = London Natural History Museum, London; GMNH = Great Northern Museum Hancock, Newcastle University; RHC = Geology Department, Royal Holloway College, University of London; KUNH= University of Kansas Natural History Museum Paleobotany Collections; ACS = Andrew C. Scott slides at Geology Department, Royal Holloway College, University of London.

Table 2, Diagnostic features of *Tetrastichia bupatides* and *Triradioxylon primaevum* fronds

Taxon Character	*Tetrastichia bupatides*	*Triradioxylon primaevum*
Vegetative branching	in one plane*	by cruciate forking**
Trace configuration	row of protoxylem strands, surrounded by more or less connected metaxylem	one or two elliptical bundles
Sclerotic hypodermis	relatively thinner	relatively thicker
Hypodermal bundles	somewhat interconnected, but often separate	usually highly interconnected, often forming continuous zone
Inner cortical parenchyma	cells with delicate walls, often not preserved	cells with less delicate walls, more commonly preserved
Black cell contents of parenchymatous ground tissues	common	rare, most often absent

* All branches in same plane, forming a two dimensionally branched frond.

**Sequential dichotomies in planes that are at right angles to each other, producing three dimensional frond.

Table 3. *Tetrastichia bupatides* frond branching and pinna data[1].

Width in x.s.	No. of lobes (protoxylems) of trace	Divergence of laterals	No. of lobes (protoxylems) in diverging lateral	Notes
5 mm	6-8	forking and with laterals (subopposite)	2	Fig. 3 of Gordon, 1938; attached rachis with pinnate branching just distal to basal fork (near stem)
2 mm	3-5, including incipient pinnule traces	alternate, 8-10 mm apart	1	"*Lyginorachis* A" of Barnard, 1960a, 9 cm long; alternate pinnules (each with single trace). *Sparganum* cortex, epidermis with possible stomata. Pinnule trace divides at level of divergence, with no *Sparganum* cortex ‖‖distal to fork.
2.5 mm	6-8, including incipient pinnule traces	subopposite, 14-15 mm apart	1	"*Lyginorachis* B" of Barnard 1960a, 7.8 cm long, subopposite pinnules (each with single trace).
~7 mm	4-5 + 4-6?	forking		Dispersed forking rachis, Fig. 23 of May and Matten, 1983
~7 mm	7 or 8?	-	-	Dispersed rachis, Fig. 25 of May and Matten, 1983
~7 mm	6-8	single lateral from rachis (opposite)	2	May and Matten's "holotype". Two attached rachises, 2 cm apart. Attached rachis 10 cm long, with one pinnate lateral (two protoxylems).
5 mm	6	opposite	1	Opposite pinnule divergence, Fig. 8c of Dunn and Rothwell, 2012
~7 mm	?	alternate	1	Subopposite pinnule divergence, Fig. 8d of Dunn and Rothwell, 2012
7 mm	6	alternate	1	Alternate pinnule divergence, Fig. 8e of Dunn and Rothwell, 2012
12 mm (oblique)	6	-	-	Fig. 3c; Attached rachis extends >3 cm without branching
1.5 > 1.0 mm	3-4	alternate	1	Fig. 2a; This is the specimen with an attached terminal aggregate pollen organ; 4 cm long below aggregate pollen organ, plus 3 cm of pollen organ. Pinnule divergence (Fig. 2e-f) is typical for *Tetrastichia*.
2.0 mm	3	alternate	1	Block 712
2.0 mm	4	alternate	1	‖
1.2 mm	3	sub-opposite	1	‖
1.5 mm	4	alternate	1	‖
2.5 mm	5	alternate	1	‖
3.0 mm	5	alternate	1	‖
1.0 mm	2	alternate	1	‖
1.5 mm	4	alternate	1	‖
1.0 mm	2	alternate	1	‖
1.5 mm	4	alternate	1	‖
2.2 mm	4	alternate	1	‖
2.0 mm	4	alternate	1	‖
2.5 mm	5	alternate	1	‖

1.5 mm	3	alternate	1	||
1.5	4	alternate	1	||
2.0 mm	4	alternate	1	||
1.0 mm	2	alternate	1	||
1.5 mm	5	alternate	1	||
1.7 mm	4	alternate	1	||
1.5 mm	4	alternate	1	||
1.7 mm	4	alternate	1	||
2.5 mm	4	alternate	1	||
2.0 mm	5	alternate	1	||
2.0 mm	4	alternate	1	||
2.0 mm	4	alternate	1	||
2.5 mm	5	alternate	1	||
3.0 mm	4	alternate	1	||
2.0 mm	5	alternate	1	||
3.0 mm	6	alternate	1	||
2.5.mm	5	alternate	1	||
2.0 mm	5	alternate	1	||
2.5 mm	5	alternate	1	||
2.0 mm	4	alternate	1	||
3.0 mm	5	alternate	1	||
2.0 mm	5	alternate	1	||
2.5 mm	5	alternate	1	||
1.5 mm	4	alternate	1	||
2.5 mm	5	alternate	1	||
2.0 mm	5	opposite	2	||
1.5 mm	3	alternate	1	||
1.5 mm	4	opposite	2	||
1.5 mm	4	alternate	1	||
2.0 mm	6	alternate	1	||
3.0 mm	6	opposite	2	||
1.5 mm	4	alternate	1	||
1.5 mm	4	alternate	1	||
1.5 mm	3	sub-opposite	1+1	||
2.5 mm	5	sub-opposite	1+1	||
2.0 mm	6	alternate	1	||
2.0 mm	5	alternate	1	||
2.0 mm	4	opposite	2	||
2.0 mm	4	alternate	1	||
2.0 mm	4	alternate	1	||
1.5 mm	4	alternate	1	||
1.0 mm	2	alternate	1	||
2.0 mm	4	alternate	1	||
2.0 mm	4	alternate	1	||
1.2 mm	4	Alternate	1	||
2.0 mm	4	sub-opposite	1+1	||
1.2 mm	3	alternate	1	||
2.0 mm	4	alternate	1	||
3.0 mm	6	alternate	1	||
2.2 mm	5	alternate	1	||

2.0 mm	5	alternate	1	||
2.0 mm	4	alternate	1	||
2.0 mm	6	alternate	1	||
2.0 mm	4	alternate	1	||
1.4 mm	5	alternate	1	||
1.5 mm	5	alternate	1	||

[1] Data from Gordon, 1938; May and Matten, 1986; Dunn and Rothwell, 2012; and new observations.

Declaration of interests

☒ The authors declare that they have no known competing financial interests or personal relationships that could have appeared to influence the work reported in this paper.

☐The authors declare the following financial interests/personal relationships which may be considered as potential competing interests: